Chapter 3

Extracellular matrix remodeling in heart with multiple stress inductions manipulated through *in-vitro*, *in-vivo* and clinical studies.

Chapter 3

Extracellular matrix remodeling in heart with multiple stress inductions manipulated through *in-vitro*, *in-vivo* and clinical studies.

A. Introduction

With more than 20 million people worldwide receiving a heart failure diagnosis for the first time, heart failure continues to be a major cause of mortality and morbidity and a public health concern.[81,97] Cardiovascular diseases (CVD) had at least 30 million cases and 50 million cases by 2016 in the US and India, respectively, with a mortality rate of over 70% in India..[82] Diabetes is an equally threating disorder that affects individuals globally. The devastating effect that diabetes implements on the cardiovascular system contributes to a large number of mortalities globally. Diabetes induced cardiac dysfunction or Diabetic cardiomyopathy is a condition that exposes the affected individual to an elevated risk of MI, atherosclerosis and Hypertensive heart disease (HHD).[132] Diabetic cardiomyopathy is characterized by left ventricular hypertrophy, fibrosis, impaired diastolic and systolic function, and an increased risk of heart failure. Extracellular matrix (ECM) remodeling in heart is one of the contributing factors of pathogenesis in cardiovascular diseases.[27,28] Cardiac ECM remodeling is a critical contributor in the progression of Left Ventricular (LV) remodeling where under-expression or breakdown of Collagen is responsible for LV dilatation whereas over deposition of Collagen leads to fibrosis.[92] In addition to Collagen-III, fibronectin, proteoglycans, matrix metalloproteinases (MMPs), and tissue inhibitors of matrix metalloproteinases (TIMPs), Collagen-I makes up the majority of the matrix interstitium of the heart. The three stages of cardiac remodeling following cardiac injury are inflammatory, proliferative and maturation phases leading to a mature scar formation.[29] The preliminary stages

of ECM remodeling are necessary as it prevents rupture of the ventricular wall as during a Myocardial Infarction, around a billion cardiac cells die. This paves way for a fibrotic scar to form and aid in the healing process., however, exacerbated ECM remodeling leads to progressive fibrosis in the heart and cardiac disfunctioning.[30,31]. A normal ECM comprises of three interconnected layers of Collagen namely- endomysium, perimysium and epimysium. Surrounding individual cardiomyocytes is the endomysium, the perimysium encases the major cardiac bundles while the epimysium encompasses the entire cardiac muscle.[90] In addition to the critical role of providing structural integrity and maintain the ventricular geometry, the matrix network also participates in signal transduction pathways to maintain the survival and function of cardiac cells. The proportion and biochemistry of the ECM change due to underlying pressure overload, cardiac injury, myocardial infarction (MI), and/or ischemia-reperfusion (I/R) injury that leads to extracellular matrix reorganization which in turn is modulated by changes in turnover of matrix proteins.[36] The matrix composition changes from synthesis and accumulation of MMPs during the inflammatory phase to the presence of huge amounts of activated myofibroblasts during the proliferative phase and finally extensive Collagen deposition and crosslinking to form a mature scar. It is also during the inflammatory phase where a provisional matrix is formed post an MI and activation PDGF, FGF and TGF families occur. Tgf-β then activates the Smad2/3 pathway which in turn is believed to activate profibrotic genes and MMPs.

A family of zinc-dependent proteases called MMPs is involved in collagen turnover..[32] MMPs possess endopeptidase function by which they degrade Collagen. In a normal heart, the turnover of Collagen i.e., the rate of synthesis of new Collagen and degradation of old strands of Collagen is strictly regulated as well as the proportion of Collagen-I/ Collagen-III is tightly regulated. It has been reported that there is rapid degradation of Collagen type-1 and extensive synthesis

of Collagen-III after MI which can continue up to a year after a MI attack.[92] Similarly patients with diabetic cardiomyopathy express significant upregulated expression of Collagen-III and IV and alloxan induced rats show an upregulated expression of Collagen-VI.[132] Expression of other matrix components like elastin, fibronectin, fibrillin, proteoglycans are altered during MI or in hypertensive heart disease.[31] Further, non-selective MMP inhibition combined with doxycycline during the early stages show a weak progression towards LV dilatation and ST-elevation MI (STEMI).[90] Interestingly, supplementing the myocardium of MI mice models with ECM components from healing zebrafish may facilitate regeneration in infarcts. The Adamts family is a significant MMP because in addition to performing MMP tasks, they also function as disintegrins. Adamts4 is a member of the Adamts family and is also known as aggrecanase-I. To date 19 members of mammalian ADAMTS proteinases have been identified with functions ranging from ECM degradation, cell adhesion and proteolysis. It is a metalloproteinase and a disintegrin with thrombospondin like motifs.[33,34] Interestingly, Adamts4 knockout animal models have been shown to survive with normal growth and without any bone remodeling.[133] Adamts4 has been known to bind to the ECM proteins and executes cleavage of ECM proteoglycans like aggrecan, versican and brevican apart from regulating collagen turnover.[35,36] TIMP3 is a potent inhibitor of Adamts4 significantly inhibits the aggrecanse activity of Adamts4.Adamts4 through degradation of matrix proteoglycans is involved in the pathogenesis of osteoarthritis and degenerative osteoarthritis by degrading aggrecan, a disease characterized by cartilage degradation.[37,38] Along with its participation in the pathophysiology of osteoarthritis, Adamts4 has also been related to angiogenesis and cancer, where its exact function is still up for debate. According to some studies, it serves as a marker for early-stage cancer, such as colorectal cancer. However, other studies suggest that its altered and shortened fragments may restrict angiogenesis to slow the growth of tumors.[39,40]

There is not sufficient information in the context of cardiac remodeling with a focus on the involvement of Adamts4. So far it is known that Adamts4 knockout in animal models leads to a reduction in plaques in cases of high fat induced atherosclerosis[41] besides that the inhibition of Adamts4 with pentosan polysulfate following aortic banding improves cardiac functioning.[36]. The baseline level of Adamts4 expression and function in the developing and adult heart, as well as in post cardiac damage, are not well understood, nevertheless. Adamts4 and Adamts1 levels continue to be increased in individuals with acute aortic dissection and coronary artery disease, according to research published very recently.[42,43]

In this study, for the first time, Adamts4 was identified as a novel biomarker of adult cardiac injury under stress conditions. To better understand the molecular insights of Adamts4 induction and associated affected signaling pathway activation, we have used H9c2, a rat ventricular myoblast cell line for several *in vitro* assays. Likewise, Adamts4 expression was induced in H9c2 cells, subjected to hypoxia (Hyp) and ROS injury inductions *in vitro*. Moreover, we manipulated the expression of Adamts4 with siRNA-mediated loss of function and TGF- β inhibitor studies in H9c2 cells to evaluate its regulation and dependency on TGF-β signaling since TGF-β has been long known to be a characteristic marker for inflammatory and fibrotic responses following pathological stress including MI, ischemia and reperfusion (I/R) injury.[44–48] Finally and most importantly, we also validated our hypothesis in human clinical samples and demonstrated the induced expression of ADAMTS4 in patients with indicated cardiac ailments. To study the role of Adamts4 in diabetic cardiomyopathy H9c2 were pre-conditioned and grown at at low concentration (5mM) supplemented glucose as the control group and the cells to be treated were grown in media supplemented with 20mM of glucose for 48 hours following which the expression of Glut1, Collagen-III and Adamts4 was studied with the help of qPCR and Western Blot. An enhanced

expression of Adamts4 indicated the involvement of Adamts4 in ECM remodeling in the context of diabetic cardiomyopathy also.

B. Methods

Human studies.

For this study, a total of seventy (70) impacted clinical samples were used. For the investigation, venous blood samples were used. IPGME&R's institutional ethics committee in Kolkata gave its ethical approval for the collection (IPGME&R/IEC/2019/517). Dilated cardiomyopathy (DCM), DCM with diabetes (DCM&D) and Myocardial Infarction (including AWMI-anterior wall MI and IWMI-inner wall MI) were chosen as two major types of cardiac diseases. Blood from healthy volunteers who were not known to have been diagnosed with any heart conditions or other lifestyle diseases made up the Control group. Table 1 lists the characteristics of the patient samples. Blood samples were collected in Sodium (Na) EDTA vials and clot vials. Histopaque was used to separate peripheral blood mononuclear cells (PBMCs) from the 2NA-EDTA vials.[134] (10771, Sigma) following the manufacturer's protocol. Following the successful isolation of PBMC, ice-cold mammalian lysis buffer (250 mM NaCl, 50 mM Tris pH 7.5, 0.1% SDS, 1% TritonX, and 5 Mm EDTA) was used to prepare for protein isolation. This buffer also contained a protease inhibitor cocktail (Genetix GX-2811AR) and a phosphatase inhibitor (Genetix GX-0211AR). Small aliquots of the proteins were kept at -80°C until they were used for Western Blotting.

Table 1

Groups	Control (*n*=10)	DCM (n= 10)	AWMI (*n*=10)	IWMI (10)	DCM&D (n=5)
Age	20-55 years	20-55 years	28-60 years	30-60 years	40-55 years
Sex, M/F	6/4	6/4	7/3	7/3	3/2
Smoker, M/F	0/0	3/0	4/0	1/1	2/0

Table 1: *Characteristics of clinical sample groups*

Cell culture studies.

On the rat ventricular cardiomyoblast cell line H9c2, all in-vitro tests were conducted. The cells were maintained at 5% levels at 37°C in a sterile humidified CO2 incubator with Dulbecco's modified Eagle's medium (AT007, Himedia) supplemented with 10% FBS (RM10409, Himedia) and 1% penicillin/streptomycin (Pen-Strep) cocktail (15140122, Invitrogen).[135] At roughly 75–80% confluency, the cells were employed for subsequent tests. Serum-free DMEM was used for the therapies that were being tested. The cells were exposed to H_2O_2 (100 uM) for one hour in order to produce ROS..[6,136] For hypoxia induction, the cells were put in an anaerobic chamber with an anaerogas pack (LE200A, Himedia) and anaero indicator tablet (LE065, Himedia) according to the manufacturer's instructions. The anaerobic chamber with cells was incubated in the CO_2 incubator for 12 hours, the indicator colour change confirmed hypoxia induction in the chamber.[137] For glucose shock treatment cells were maintained at low concentration (5mM) supplemented glucose as the control group and the cells to be treated were grown in media supplemented with 20mM of glucose for 48 hours. Murine adult primary mice cardiac fibroblasts

were isolated and maintained in cell culture as described previously[138] on collagen coated plates. For primary cardiomyocyte culture, protocol described previously[139] was followed except for the Langendorff perfusion set-up which was replaced by mechanical perfusion set-up. The cells were used for further experiments at about 75-80% confluency. For experimental treatments, serum-free media was used.

Animal study and experimentation

All experiments and protocols involving animals were reviewed and approved by the Institutional Animal Ethics Committee of Presidency University, (PU/IAEC/SC/39). Male Wistar rats, aged 22-24 weeks were used for this study. Animals were fed with high fat diet for 6 weeks (water was provided *ad libitum*) to induce pre-disposition to Type-2 diabetes (T2D) and fasting blood glucose (FBG) was checked every week with the help of Accucheck glucometer strips (Roche diagnostics) following which intraperitoneal administration of Alloxan monohydrate (ab 143569, Abcam) at 150 mg/kg dosage and Control group was a similar age and sex matched. The control group was fed with a standard chow diet. Rats with a maintained 200mg/dl FBG were taken as successful diabetic model system. Along with FBG, serum cholesterol and triglycerides were also measured by a colorimeter assay.

Serum Triglyceride and Cholesterol measurement

Serum was obtained from rat tail after letting the blood clot, the serum was carefully aspirated and placed in another tube. Serum Triglyceride was measured using a kit based on the classic GPO (glycerol phosphate oxidase) (Erba,121175) method and CHOD-POD (cholesterol oxidase and peroxidase) method for Cholesterol (Erba, 120194) assays. The absorbance was recorded at 546nm and 505 nm for measuring triglycerides and cholesterol against a given standard. Instructions were followed according to manufacturer’s protocol.

TGF-β inhibitor, SB431542 and siRNA treatment.

For the purpose of inhibiting TGF-, the cells were pre-treated for 30 minutes with the strong ALK inhibitor SB431542 (ab120163, Abcam), before being exposed to H_2O_2 and the previously reported hypoxia induction.[48] For the purpose of knocking down Adamts4, cells were transfected with Adamts4 siRNA (ATSsiRNA) (50 pmol) (4390771, Ambion) and Lipofectamine RNAiMax reagent (13778-075, Invitrogen) after an overnight serum starvation when they were at least 70% confluent for 48 hours. Scrambled siRNA (silence select negative control no 1 siRNA) (4390843, Ambion) (scsiRNA) was utilized as a negative control. Following a 48-hour treatment with Adamts4 siRNA, the cells underwent the same H_2O_2 and hypoxia treatments as previously mentioned.

RNA isolation, RT-PCR, and real-time PCR.

Total RNA was extracted using the Trizol-Chloroform technique from untreated and treated H9c2 cells. The Biorad cDNA synthesis kit was used to create cDNA from 1 μg of total RNA. (iScript™ Reverse Transcription Supermix for RT, 170-884) in 20 μl of total volume according to manufacturer's protocol. The cDNA prepared was used for primer optimization using DNA Taq polymerase (by RT-PCR in reverse time for real-time PCR against primers (BIOTAQ DNA polymerase BIO-21040, Bioline,). The rodent primer pairs adamts4, hif-1α, β-actin, catalase, Tgf-β1, collagen-III, α-SMA and glut-1 were used in 35 cycles of PCRs. Real-time PCR experiments also made use of these primer pairs. The Bio-Rad real-time PCR kit (172-52 03AP, SSO quick Eva green super mix) was used to perform the real-time PCR. With β-actin, the gene expression of the aforementioned genes was normalised.

Protein Isolation and Western Blotting.

Using the aforementioned ice-cold mammalian lysis solution, protein isolation was carried out. Western blotting was carried out in the manner previously mentioned.[107] According to previously reported procedures, the immunoblots were created using ClarityTM Western ECL substrate (1705060, Bio-Rad) and scanned using ChemiDoc MP (Bio-Rad).[108] The antibodies used were Adamts4 (PA1-1749A, Invitrogen) used at a concentration of 2 μg/ml, α-SMA (14-976082, Invitrogen) used at a dilution of 1:500 and Tgf-β1 (ab64715, Abcam,) used at a concentration of 1 μg/ml. To determine total protein intensities, the SDS gels were also stained with 2.5% coomassie (Brilliant blue G, SRL) and destained with coomassie de-stainer. The previously described ChemiDoc MP was used to scan the coomassie stained gels. With the use of the ImageJ program from the NIH, intensities were quantified.

Immunostaining.

H9c2 cells were immunostained using the previously described procedure. [6] Following the previously described methodology, immunostaining was carried out in H9c2 cells with the exception of the absence of the permeabilization stages for staining with antibody Adamts4 (PA1-1749A, Invitrogen) used as earlier, Tgf-β (ab64715, Abcam) was employed at a concentration of 2 μg/ml, along with α-SMA (14-976082, Invitrogen) and Collagen III (ab 7778, Abcam) both used at 1:400 and 1:1000 dilution respectively, Periostin (ab14041, Abcam), at a dilution of 1:500. The corresponding secondary antibodies Alexa flour 488 anti-rabbit secondary antibody (ab150077, Abcam) and Alexa flour 594 anti-mouse secondary antibody (ab150116, Abcam) were added against their respective primary antibodies after an overnight incubation at 4°C with these primary antibodies. DAPI (SRL, 18668) was used to label the nuclei of every cell. LasX

software and a Leica confocal microscope were used to capture the images. Using ImageJ software, the fluorescence intensities were measured and quantified.

Enzyme linked immunosorbent assay (ELISA)

To carry out ELISA, an ELISA kit (ab213753, Abcam) was employed. Samples were placed onto the wells in duplicate after serum proteins were diluted with sample buffer in a ratio of 1:10 to the samples. ELISA was carried out in accordance with the manufacturer's instructions.

Statistical Analysis

The statistical analysis was carried out using the GraphPad Prism 9.3.1 program. The mean and standard deviation of the mean (SD) or the median, quartiles, and range are used to represent each outcome. Student's unpaired two-tailed T-tests and one-way ANOVAs were used in the statistical analyses for groups with more than two. For $p < 0.05$, differences between the groups were deemed statistically significant.

C. Results

H9c2 cell morphology after ROS and Hypoxia injury induction. The change in morphology with reduction in size of H9c2 cells subjected to H_2O_2 and hypoxia as compared to control group is depicted by Phalloidin immunostaining in Fig. 1a. Staining with Alexafluor conjugated Phalloidin validated the reduction in cell size after both injury inductions. A reduction in cell size from 260 μm^2 for the control group to 180 μm^2 and 170 μm^2 for H_2O_2 and hypoxia treatment groups respectively (Fig. 1a and b).

Figure 1

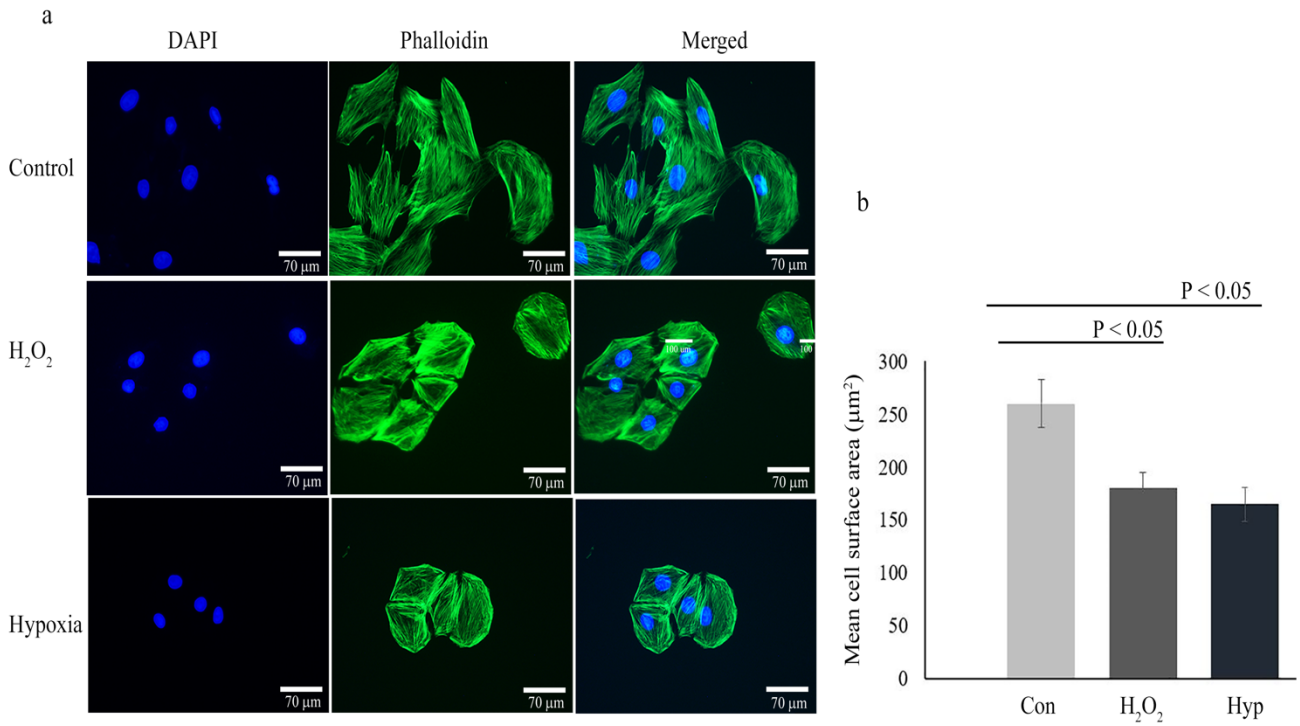

[***Figure 1: H9c2 Cell morphology after ROS and hypoxia injury.*** *Immunostaining with Alexa fluor conjugated Phalloidin showed reduction in cell size from 260 µm² for the control group to 180 µm² and 170 µm² for H_2O_2 and hypoxia treatment groups respectively (shown in panel a and b). n=3, data analyzed and expressed as mean ± SD. Differences were considered statistically significant for p < 0.05.]*

Adamts4, Tgf-ß1 upregulation in H9c2 cells following H_2O_2 and Hypoxia treatment. H9c2 cells were subjected to H_2O_2 and Hypoxia treatment. Figs 1a and b show upregulation of ROS and hypoxia injury associated markers: Catalase[6,135,136] and Hif-1α[140] respectively, quantified by qPCR (Fig. 2a and b). Also, Collagen-III[141,142] mRNA levels quantified by real-time PCR show an enhanced expression in both the stress treated groups (Fig. 2d). Also, Tgf-β1

mRNA levels follow similar pattern of expression under both the treatment conditions. PCR (Fig. 2e). Further, Adamts4 expression at both mRNA (Fig. 2c) and protein levels (Fig. 2 f and g) assessed by western blot (WB) show a significant upregulation following hypoxia and H_2O_2 treatments. α-SMA also followed the same trend (Figs. 2 f and h). Vimentin, a type-III intermediate filament marker known to promote mesenchymal cell repair following severe stress or injury to cells to initiate wound healing [143,144] was also found to be elevated in both hypoxia and H_2O_2 treated groups (Fig. 2f and i). This figure shows the upregulation of ECM markers like α-SMA, Col-III, Vimentin along with Adamts4 and Tgf- β1 post H_2O_2 and Hypoxia treatment. All qPCRs were normalized with β-actin and total protein was used as loading control for western blot assays.

Figure 2

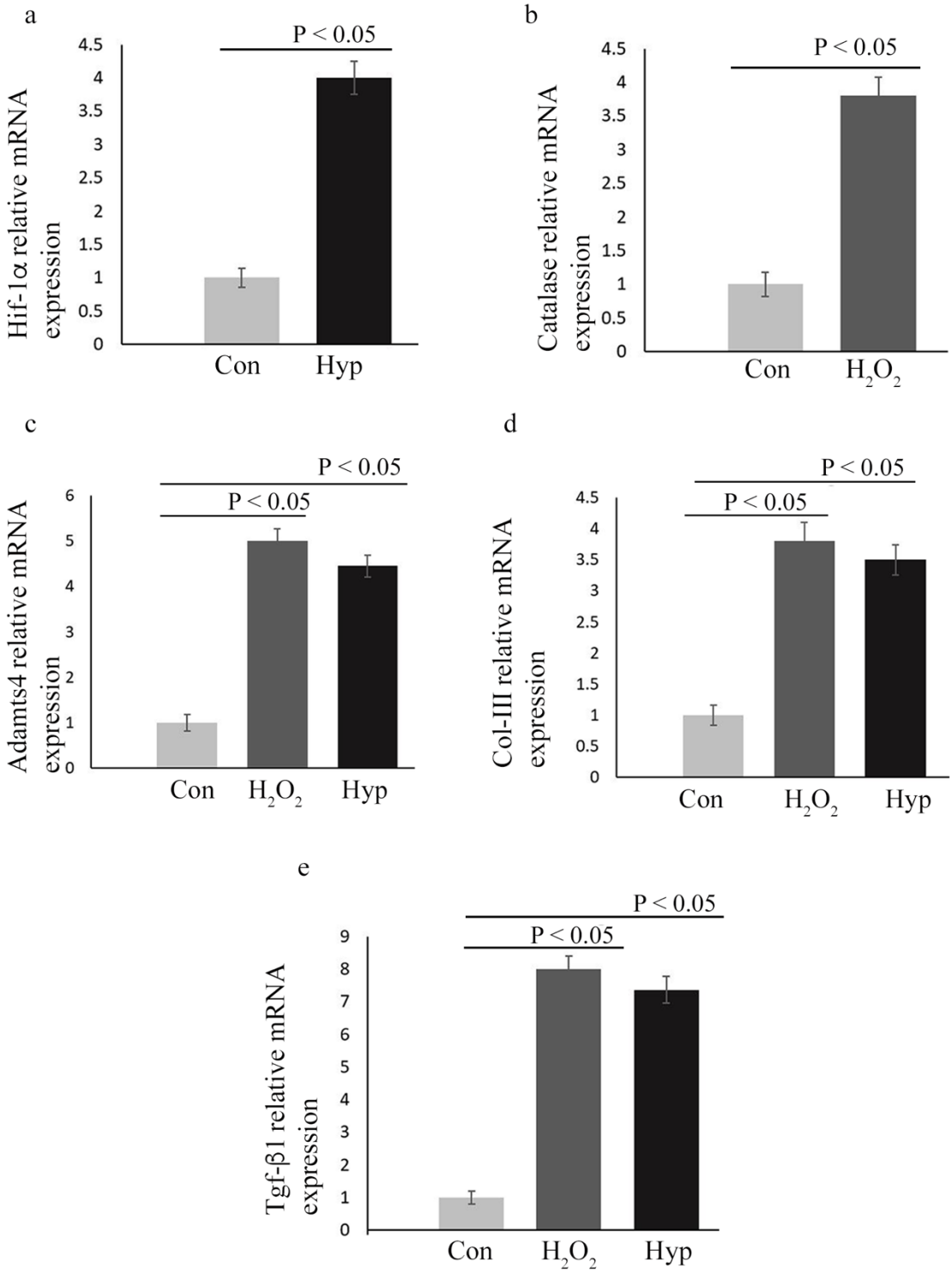
a
P < 0.05
Hif-1α relative mRNA expression
4.5
4
3.5
3
2.5
2
1.5
1
0.5
0
Con
Hyp
b
P < 0.05
Catalase relative mRNA expression
Con
H2O2
c
P < 0.05
P < 0.05
Adamts4 relative mRNA expression
6
5
4
3
2
1
0
Con
H2O2
Hyp
d
P < 0.05
P < 0.05
Col-III relative mRNA expression
Con
H2O2
Hyp
e
P < 0.05
P < 0.05
Tgf-β1 relative mRNA expression
9
8
7
6
5
4
3
2
1
0
Con
H2O2
Hyp

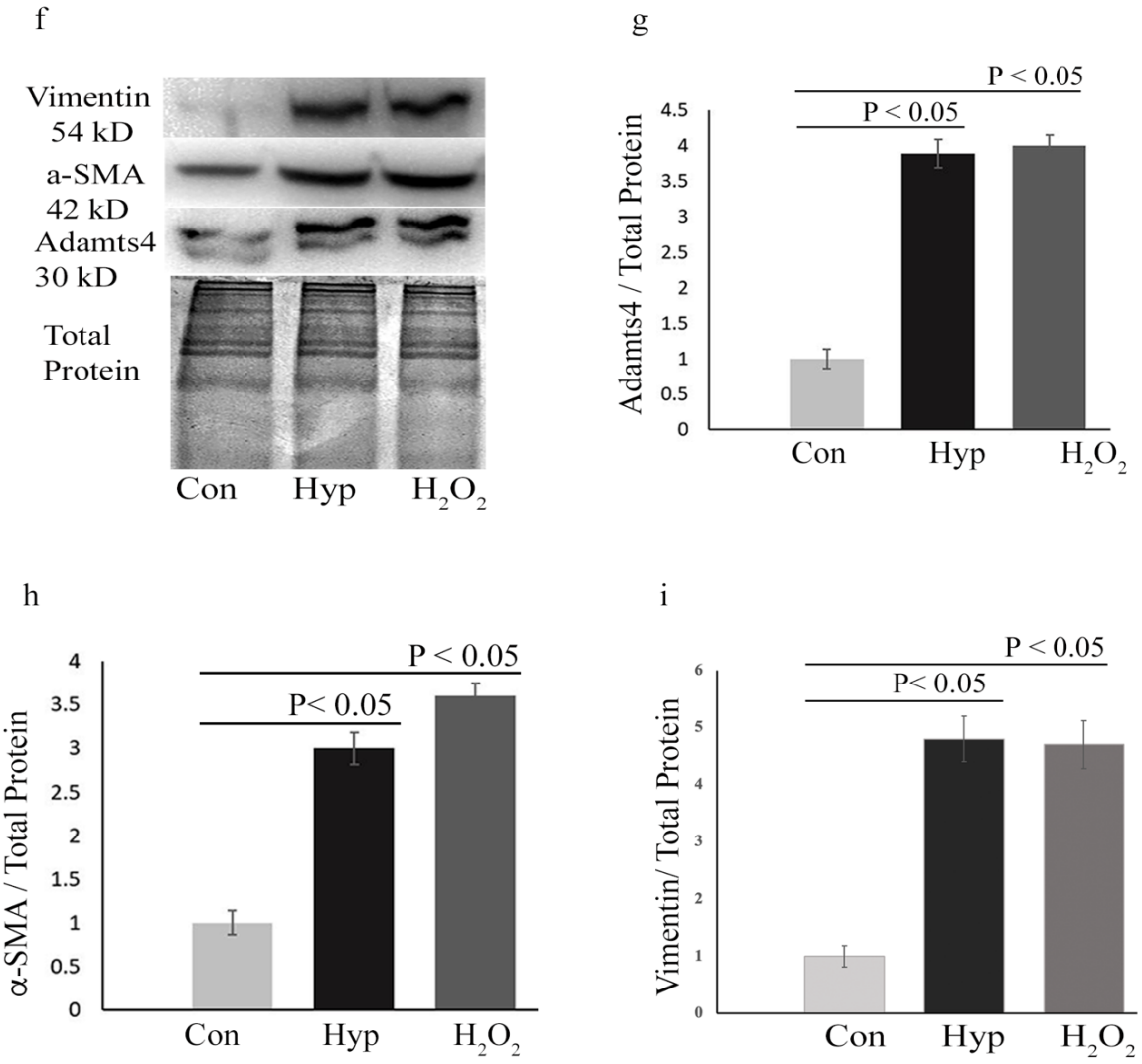

[*Figure 2: Injury induced overexpression of Adamts4 and fibrosis related markers in H9c2 cells*. *Relative mRNA expression assessed by quantitative real-time PCRs of Catalase (a) shows an upregulation by 3.8 fold, Hif-1α (b) was found to be elevated by 4 fold, Adamts4 (c) was found to be upregulated by 5 and 4.5 fold for H_2O_2 and Hyp treatment sets respectively, Col-III (d) was found to be elevated by 4 and 3.5 fold H_2O_2 and Hyp treatments, Tgf- β1(e) levels were upregulated by 8 and 7.4 folds for H_2O_2 and Hyp treatments respectively. Also, elevated expression of proteins analyzed by WB with Adamts4 (f and g) showed an enhanced expression of 3.7 and 4-fold for Hyp and H_2O_2 treatments, α-SMA (f and h) showed an upregulation of 3 and 3.5 folds Hyp and H_2O_2 treatment*

groups, Vimentin (f and i) under stress induced conditions of hypoxia and H_2O_2 showed upregulated expression by 4.8 fold for hypoxia and 4.7 fold for H_2O_2 treatments. Elevated expression of markers- Catalase and Hif-1α signified successful injury inductions while upregulated expressions of Adamts4, Col-III, Tgf- β1, α-SMA and Vimentin indicated development of injury related fibrosis. β-actin was used to normalize gene expression for qPCR assay and total protein was used as loading control for WB. n=3. Data analyzed and expressed as mean ± SD. Differences were considered statistically significant for $p < 0.05$]

Inhibition of Tgf-β1 and Adamts4 expression by SB431542 (ALKI) pre-treatment prior to H_2O_2 and Hypoxia stress induction. anti-Adamts4 and anti-Tgf-β1 antibody staining showed an enhanced expression of both the markers following H_2O_2 and Hypoxia treatment. A significant increased fold change of 4 and 3.7 in the fluorescence mean intensity of Adamts4 expression following H_2O_2 and Hypoxia treatments was observed which reduced significantly in presence of ALKI pre-treatment (Figs. 3a and b) in comparison to control. Further, the WB also shows a similar trend in the expression pattern of Adamts4 protein with an enhanced expression for the Hyp, H_2O_2 treated groups that reduced drastically for ALKI + Hyp and ALKI + H_2O_2 treated groups (Figs. 3d and e). Also, Tgf-β1 IF shows a similar trend with an enhanced expression of Tgf-β1 observed in H_2O_2 and Hypoxia treated groups was significantly reduced in ALKI + H_2O_2 and ALKI + Hyp treatment group (Figs. 3a and c). Tgf-β1 levels were assessed at both mRNA and protein levels (by WB) following SB431542 (ALKI) pre-treatment.Finally, the elevated level Tgf-β1 also showed a decline in its expression for both H_2O_2 and Hypoxia subjected cells pre-treated with ALKI (ALKI + H_2O_2 and ALKI + Hyp) (Fig. 3f and g) depicted by WB. This observation is indicative of Tgf-β1 dependent activation of Adamts4.

Figure 3

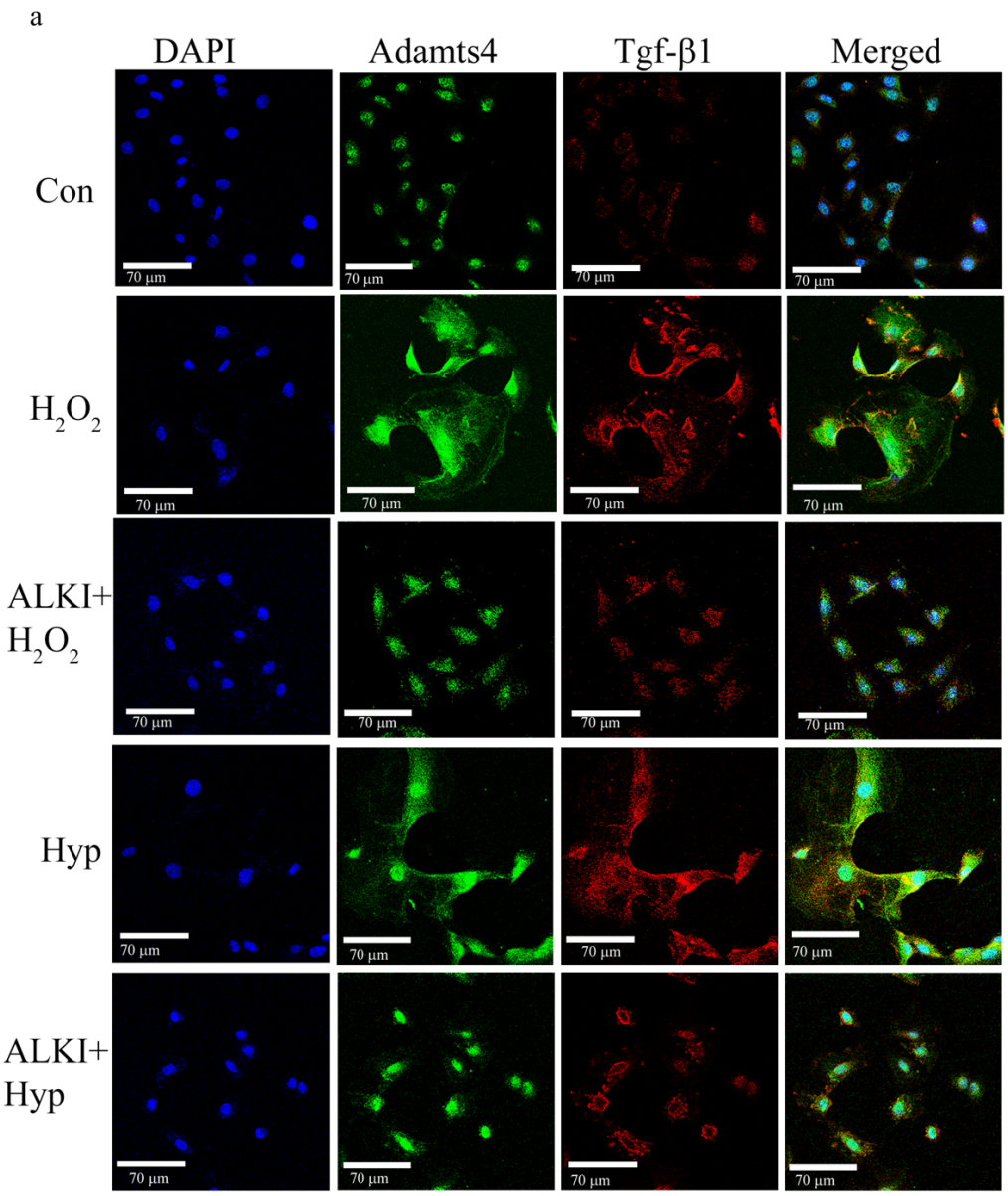
a
DAPI
Adamts4
Tgf-β1
Merged
Con
H2O2
ALKI+ H2O2
Hyp
ALKI+ Hyp
70 μm

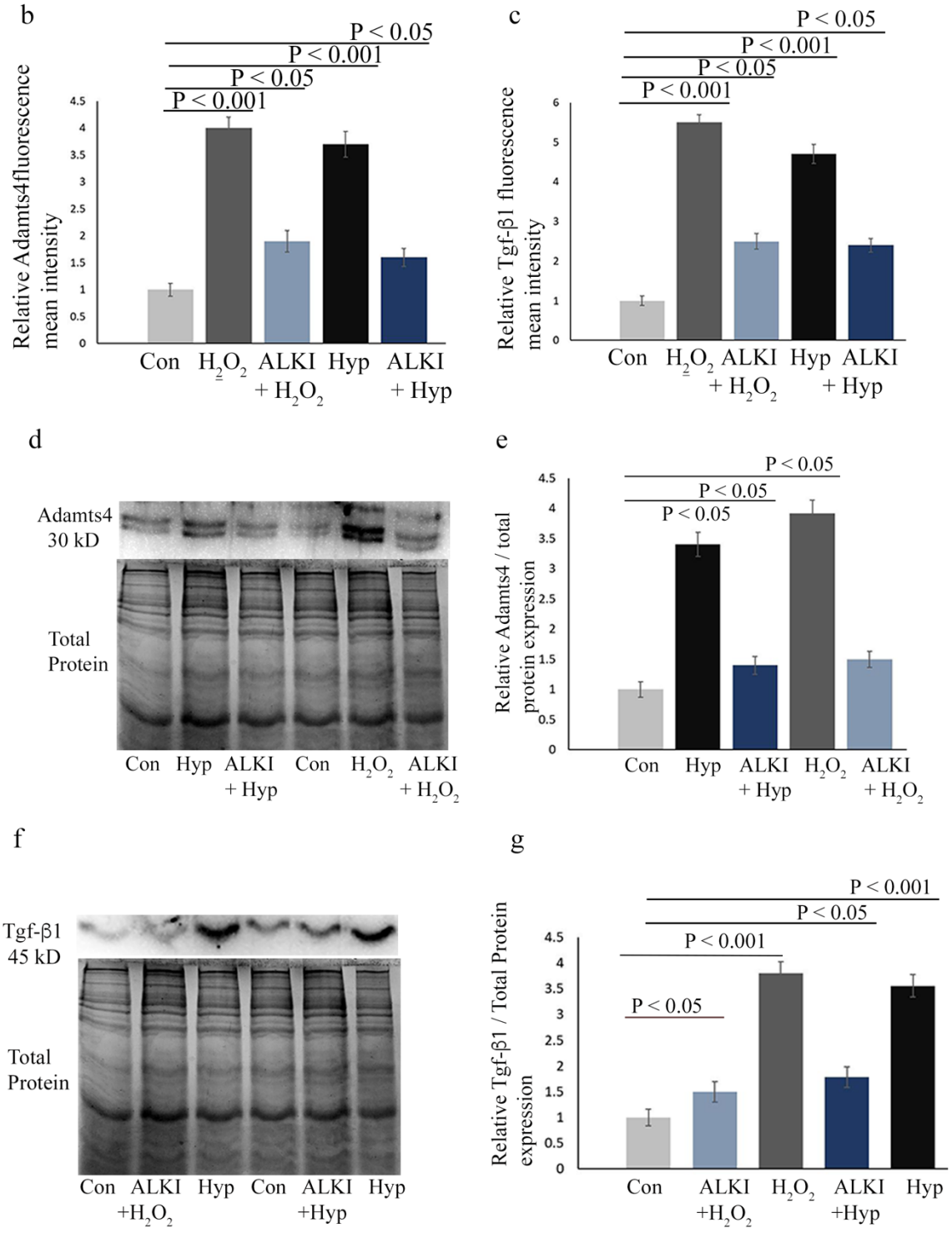

[*Figure 3: Adamts4 and Tgf- β1 expression is inhibited following pre-treatment with ALKI.* *Staining with anti-Adamts4 (shown in green) showed a 4-*

and 3.7-fold increase following H_2O_2 and hypoxia treatments in the fluorescence intensities of Adamts4 but was found to reduce to 2 and 1.6 folds in the treatment groups - ALKI + H_2O_2 and ALKI + Hypoxia respectively (a and b). IF with anti-Tgf- β1 antibody (shown in red) showed elevated expression of 4.5 and 4 fold following H_2O_2 and hypoxia treatments and this reduced to 2.5 and 2.3 folds for ALKI + H_2O_2 and ALKI + Hypoxia groups (a and c). DAPI (in blue) was used as nuclear stain. Adamts4 WB shows of increased expression of 3.7 and 4 folds for the Hyp, H_2O_2 treated groups which reduce to 1.7, and 1.5 in ALKI + Hyp and ALKI + H_2O_2 treated groups (d and e). Tgf- β1 protein expression measured by WB (f and g) showed a 4- and 3.8-fold increased change for H_2O_2 and Hypoxia subjected H9c2 cells to 1.5 and 1.8 folds for ALKI + H_2O_2 and ALKI + Hyp treatment respectively. β-actin was used to normalize gene expression for qPCR assay and total protein was used as loading control for WB. n=3, data analyzed and expressed as mean ± SD. Differences were considered statistically significant for $p < 0.05$. **]**

ALKI pre-treatment before H_2O_2 and Hypoxia treatment suppresses the expression of Collagen-III and α-SMA. Immunostaining with Collagen-III (Col-III) and α-SMA, known fibrosis markers[141,145,146] show a reduction in expression of both markers in H_2O_2 and Hyp groups pre-treated with ALKI (Fig. 4 a, b and c) as determined by measuring fluorescence intensities via ImageJ software. The elevated expression of both Col-III and α-SMA recorded after H_2O_2 and Hyp treatment significantly drops when the cells are pre-treated with ALKI. Overall, this finding is suggestive that the expression of Collagen-III and α-SMA may be Adamts4 and Tgf- β1 dependent.

Figure 4

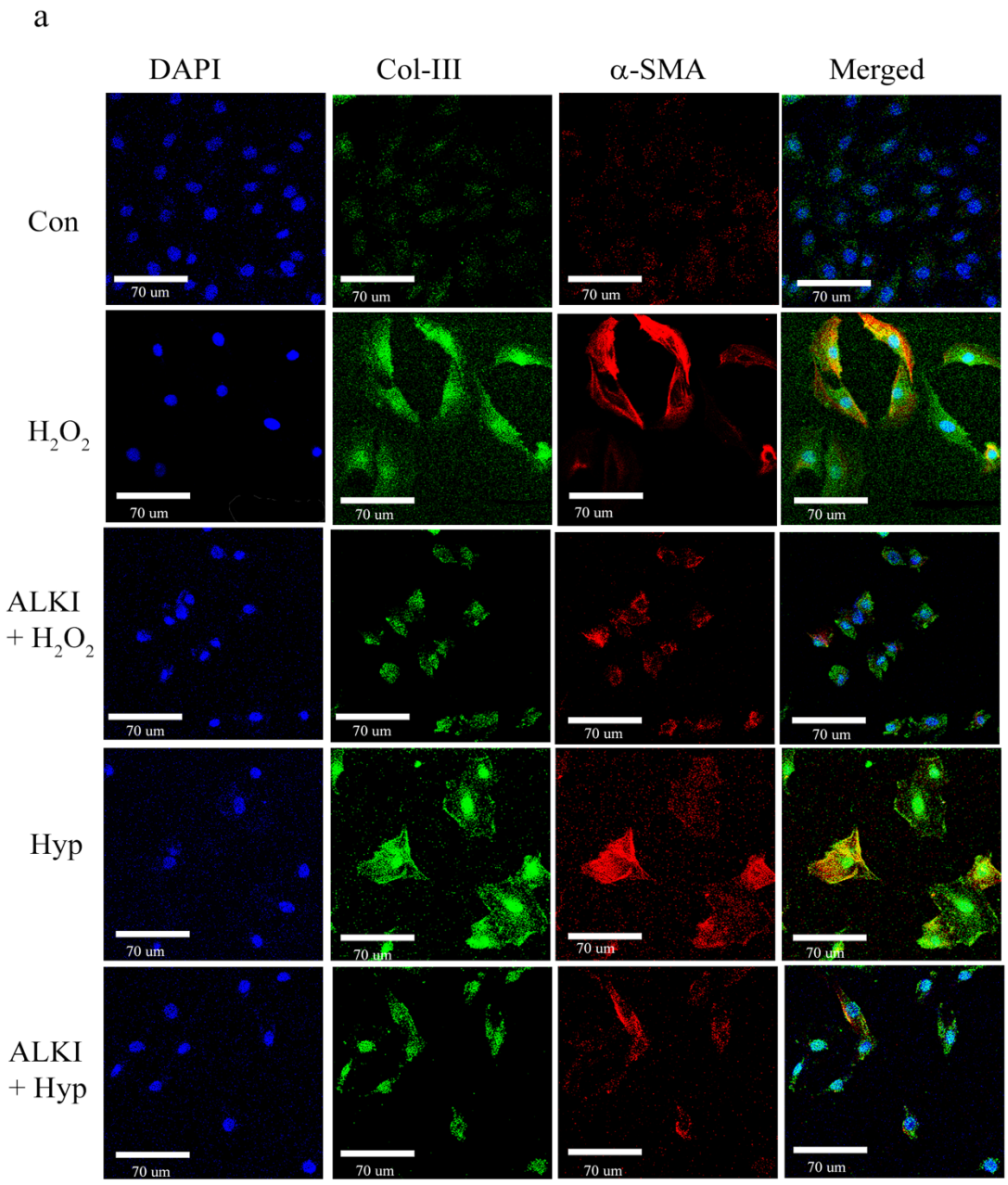
a
DAPI
Col-III
α-SMA
Merged
Con
H2O2
ALKI + H2O2
Hyp
ALKI + Hyp
70 um

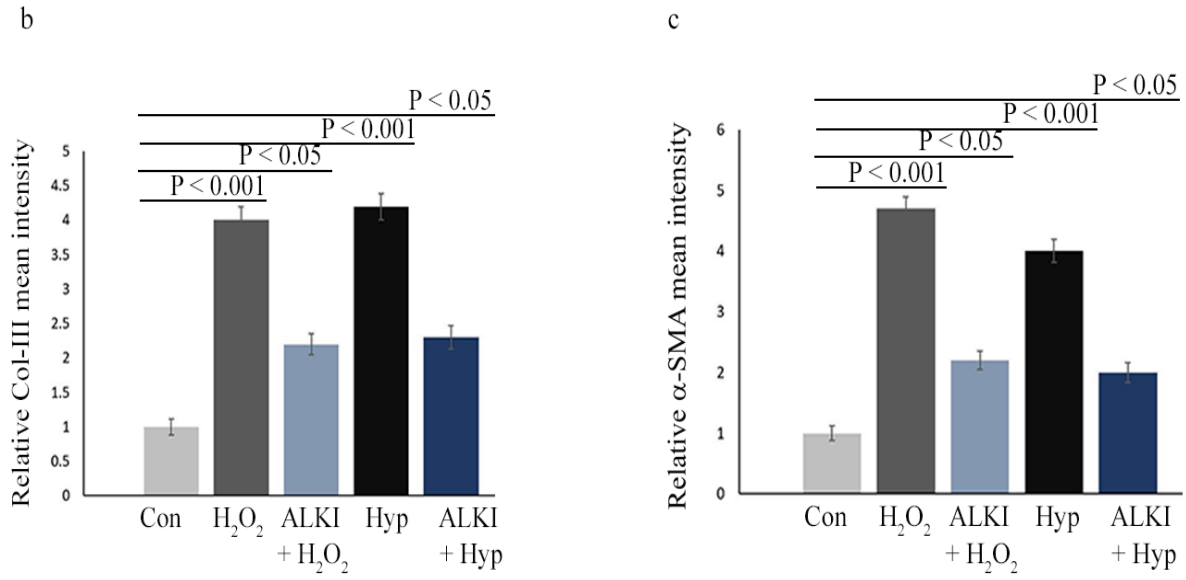

[*Figure 4. Inhibition of Col-III and α-SMA by ALKI pre-treatment.* *IF staining with anti-Col-III (shown in green) and anti-α-SMA (shown on red) antibodies showed inhibited expression of the markers under conditions of ALKI pre-treatment paired with H_2O_2 and hypoxia when compared to only injury states-H_2O_2 and hypoxia. Col-III expression reduced to 2.3 and 2.4 folds for ALKI + H_2O_2 and ALKI + Hypoxia treatment sets from 4 and 4.25 folds for H_2O_2 and Hyp treatments respectively (a and b). α-SMA levels were reduced to 2.3 and 2 folds for ALKI + H_2O_2 and ALKI + Hypoxia treatment groups from 4.6 and 4 folds for H_2O_2 and Hyp treatments respectively. DAPI (shown in blue was used as nuclear stain) n=3, data analyzed and expressed as mean ± SD. Differences were considered statistically significant for $p < 0.05$.*]

ALKI pre-treatment prior to H_2O_2 and Hypoxia treatment inhibits Periostin expression. Anti-Periostin antibody IF staining is used to detect the expression of periostin, which was found to be upregulated in the H_2O_2 and Hyp treated groups when compared to the control set.. This elevated expression of Periostin is significantly decreased in the ALKI + H_2O_2 and ALKI + Hyp groups when compared to the control group (Fig. 5a and b). WB verified the loss of function

of Adamts4 caused by Adamts4 siRNA transfection (ATSsi Tr). (Fig. 5c and d) which shows downregulation in Adamts4 expression compared to the scrambled siRNA (Scsi Tr) treated group. Total protein was used as loading control. Similarly, *Adamts4* qPCR also validated successful knockdown at the gene level (Fig. 5e). Finally, Adamts4 gene knockdown was also validated by Adamts4 IF (Fig. 5g and h). These findings collectively imply that Periostin activity may be dependent on Tgf-β1 and Adamts4, as well as effective suppression of Adamts4 mRNA in cultured H9c2 cells.

Figure 5

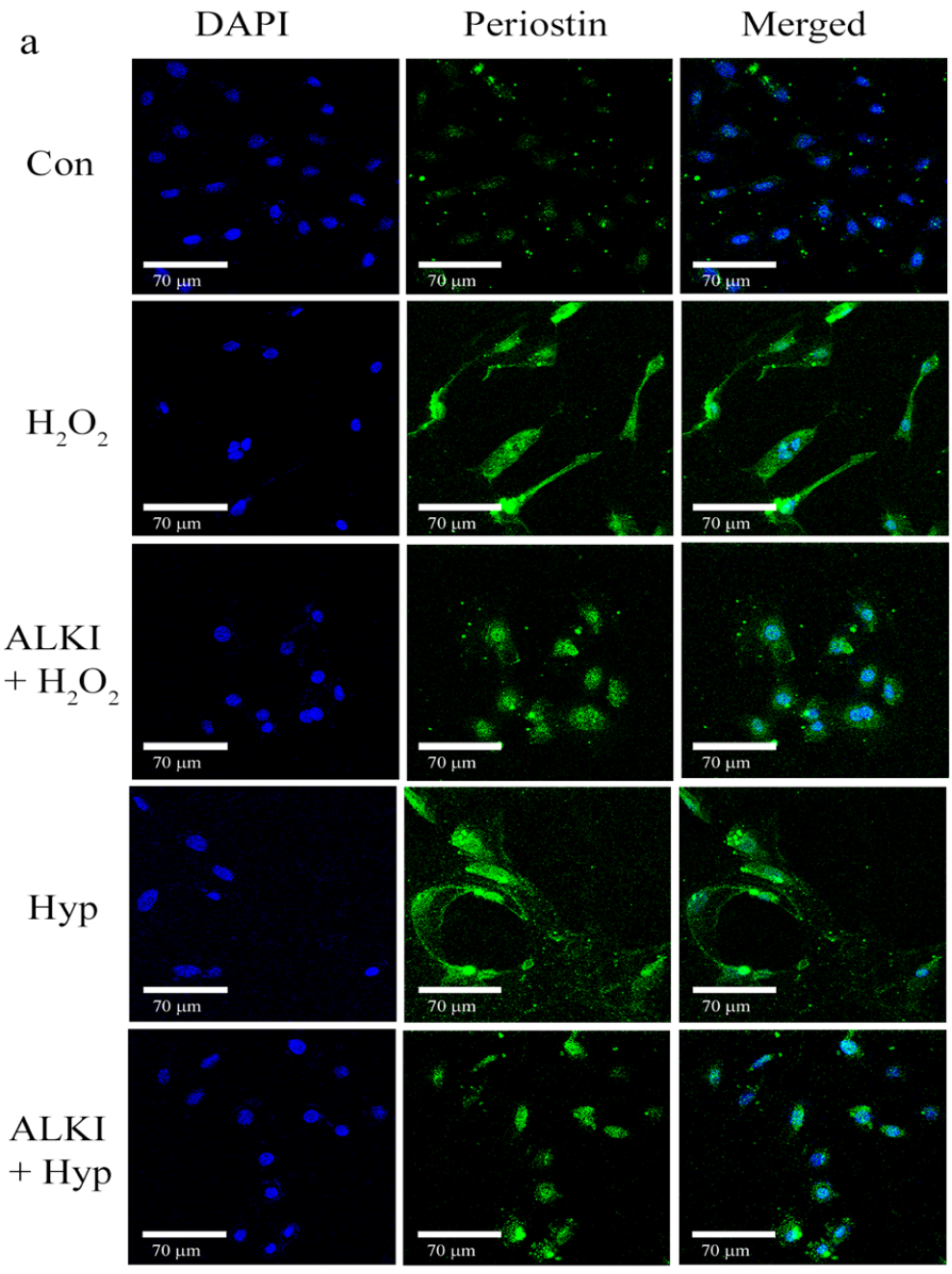

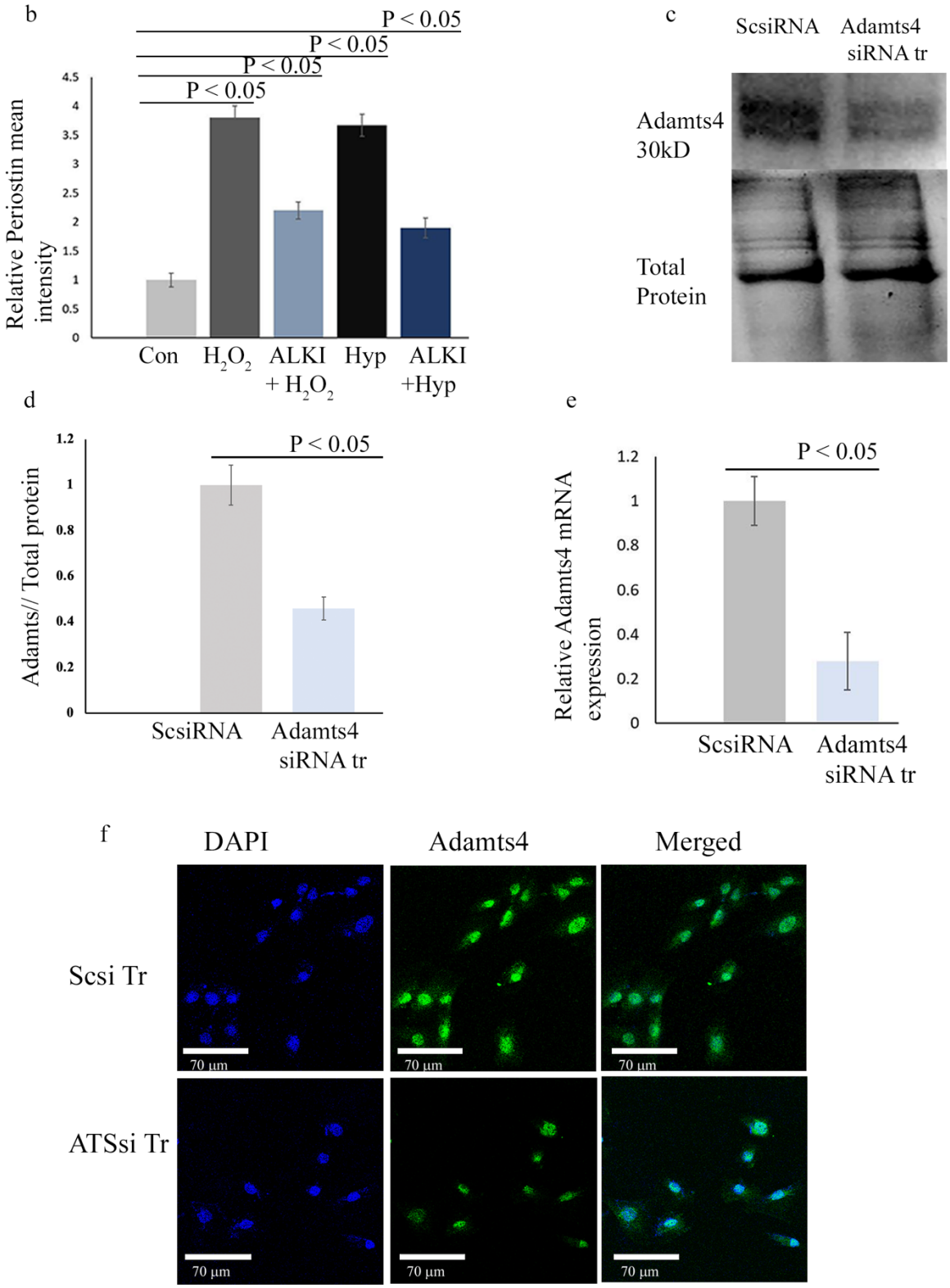
b
P < 0.05
P < 0.05
P < 0.05
P < 0.05
Relative Periostin mean intensity
4.5
4
3.5
3
2.5
2
1.5
1
0.5
0
Con
H2O2
ALKI + H2O2
Hyp
ALKI +Hyp
c
ScsiRNA
Adamts4 siRNA tr
Adamts4 30kD
Total Protein
d
P < 0.05
Adamts// Total protein
1.2
1
0.8
0.6
0.4
0.2
0
ScsiRNA
Adamts4 siRNA tr
e
P < 0.05
Relative Adamts4 mRNA expression
1.2
1
0.8
0.6
0.4
0.2
0
ScsiRNA
Adamts4 siRNA tr
f
DAPI
Adamts4
Merged
Scsi Tr
ATSsi Tr
70 µm

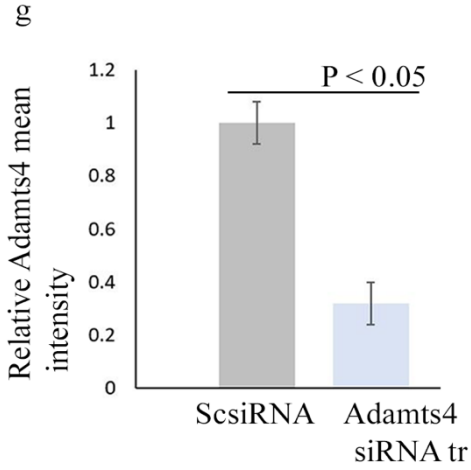

[***Figure 5. Periostin expression is reduced after ALKI pre-treatment and successful knockdown of Adamt4 mRNA in cultured H9c2 cells.*** *IF with anti-Periostin antibody (shown in green) shows inhibition of Periostin expression under ALKI + H_2O_2, and ALKI + Hyp conditions as compared to only H_2O_2 and Hyp treated conditions. A reduced expression of 2.3 and 2 folds for ALKI + H_2O_2, and ALKI + Hyp was observed which was a decrease from the 4 and 3.7 fold change found for only H_2O_2 and Hyp treatments (a and b) in comparison to control. Successful knockdown of Adamts4 via Adamts4 siRNA transfection is shown by Adamts4 WB (shown in c and d), a 0.46 fold expression in the knockdown group against the control group was found. Adamts4 mRNA levels (assessed by qPCR) were downregulated from 1-fold observed for Scsi tr set to 0.25-fold for ATSsi tr group (e). .Further, Adamts4 IF (shown in green) also validated the successful knockdown of Adamts4. A decrease in the mean fluorescence intensity from 1 as observed for Scsi treatment set to 0.33 for ATSsi tr group was found. DAPI (shown in blue) was used as nuclear stain. (f and g). n=3, data analyzed and expressed as mean ± SD. Differences were considered statistically significant for $p < 0.05$.* **]**

Adamts4 siRNA mediated gene knockdown before injury induction inhibits Adamts4 but does not affect Tgf-β1 expression. To study the regulatory hierarchy and interaction between Tgf-β signaling and Adamts4; Adamts4 knockdown experiments were performed. As expected, Adamts4 gene knockdown prior to H_2O_2 (ATSsi + H_2O_2) and hypoxia (ATSsi + Hyp) treatment showed a significant decline in the levels of Adamts4 expression as shown by Adamts4 immunostaining (Fig. 6a and b), but interestingly Tgf-β1 protein expression (Fig. 6a and c) remained largely unaffected. These finding hints that Tgf-β1 acts upstream of Adamts4.

Figure 6

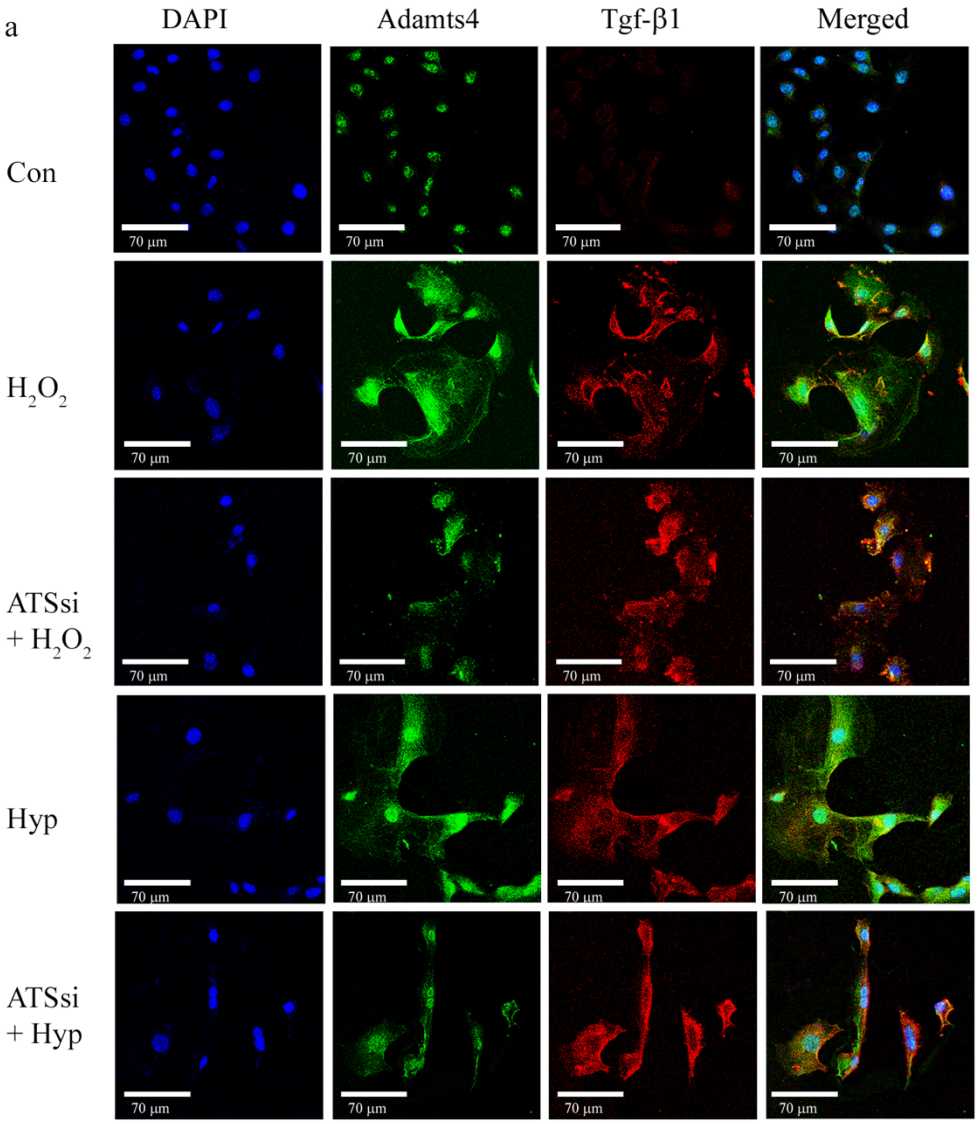

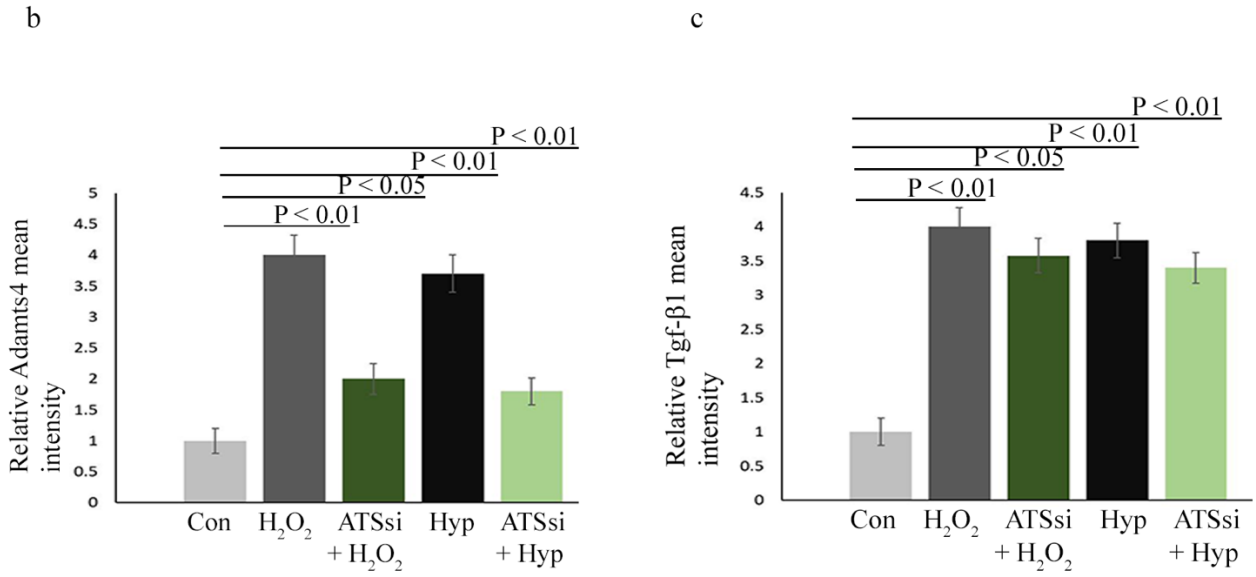

[*Figure 6: Tgf- β1 expression remains unaffected by Adamts4 knockdown.* *IF with anti-Adamts4 (shown in green) showed downregulation of Adamts4 following Adamts4 loss of function along with injury treatments. Adamts4 levels were found to decrease to 2 and 1.8 folds in the ATSsi + H_2O_2 and ATSsi + Hyp groups in comparison to the 4 and 3.7 folds increase observed for only H_2O_2 and Hyp treatments (a and b) but Tgf- β1 remained largely unaffected by this loss of function of Adamts4 and as shown by staining with anti-Tgf- β1(shown in red) where the levels of Tgf- β1 were 4.5 and 4.0 for H_2O_2 and Hyp groups and 4.2 and 4.1 for ATSsi + H_2O_2 and ATSsi + Hyp groups (a and c). DAPI (shown in blue) was used as nuclear stain. Differences between groups H_2O_2 and ATSsi + H_2O_2, and Hyp and ATSsi+ Hyp were not found to be significant. n=3, data analyzed and expressed as mean ± SD. Differences were considered statistically significant for $p < 0.05$.*]

Adamts4 loss of function (LOF) leads to inhibited expression of Collagen-III and α-SMA. Following up, the expression of fibrosis related markers is determined in Adamts4 dependent manner. Adamts4 LOF resulted in reduced expression of proteins, Collagen-III and α-SMA in groups where Adamts4 knockdown was performed before H_2O_2 and hypoxia treatment as compared to groups where only injury induction (H_2O_2 and hypoxia) was done as depicted by Collagen-III and α-SMA immunostaining (Fig. 7a). The increased expression of both Collagen-III and α-SMA observed in H9c2 cells treated with ROS and Hyp drastically reduced after Adamts4 knockdown (Fig 7a, b and c). Overall, these findings are suggestive of an Adamts4 dependent activity under stress conditions induced in the H9c2 cells.

Figure 7

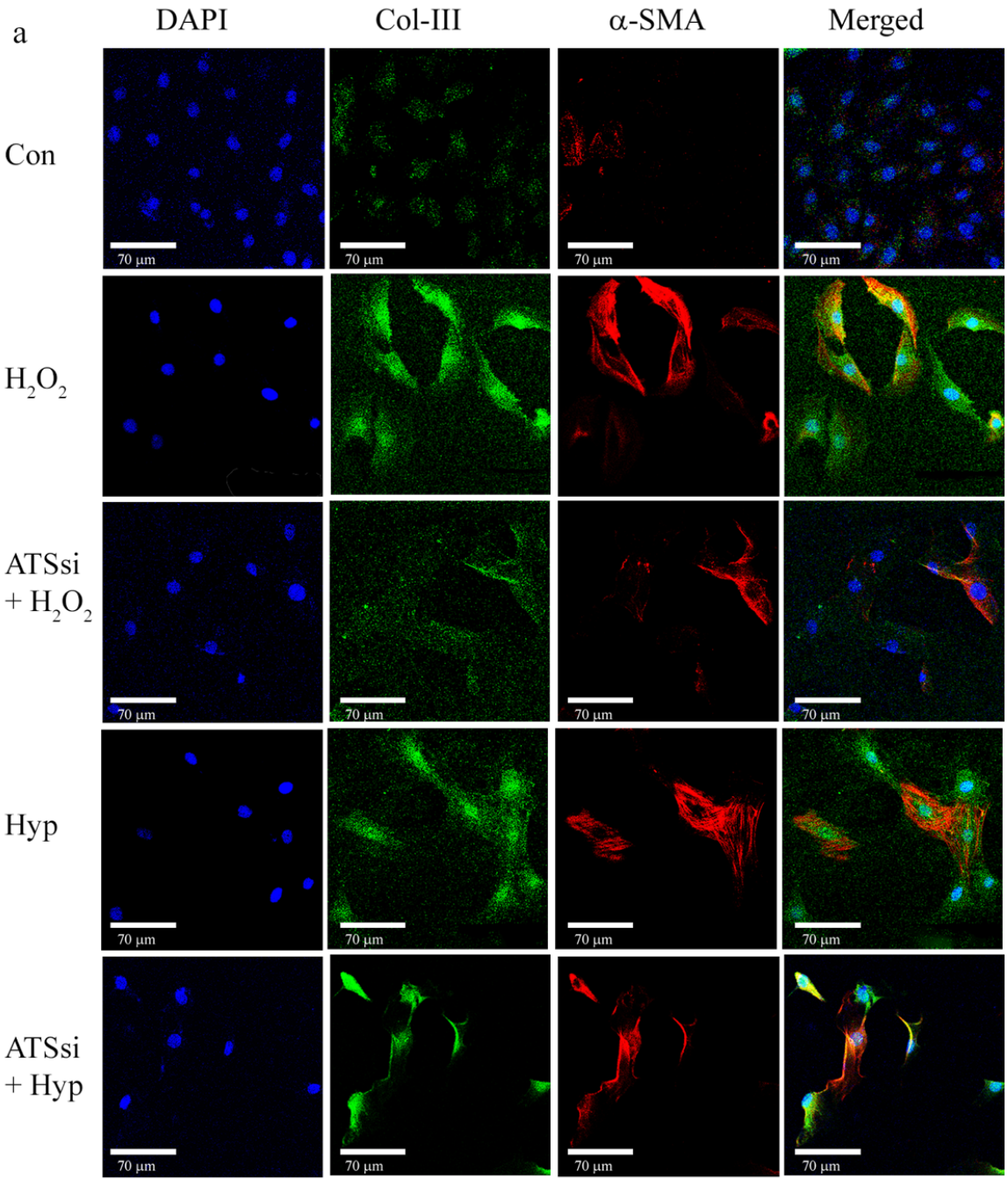
a
DAPI
Col-III
α-SMA
Merged
Con
H2O2
ATSsi
+ H2O2
Hyp
ATSsi
+ Hyp
70 μm

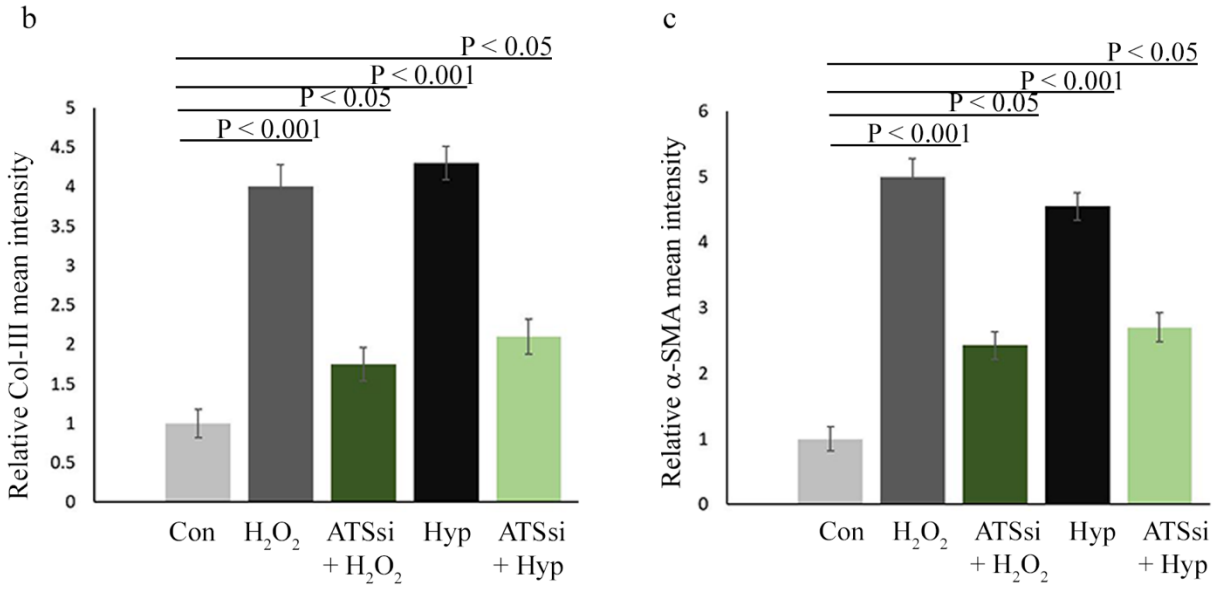

[*Figure 7: Inhibited expression of Col-III and α-SMA following loss of function of Adamts4.* *IF with anti-Col-III (shown in green) and anti-α-SMA (shown in red) antibodies show inhibited expression of these markers under ATSsi + H_2O_2 and ATSsi + Hyp conditions when compared with H_2O_2 and Hyp treated cells (a) Col-III showed a reduction from 4 and 4.25 fold observed for the H_2O_2 and Hyp treatment groups in comparison with the control group to 1.8 and 2.2 fold observed in ATSsi + H_2O_2 and ATSsi + Hyp groups (a and b). Similarly, for α-SMA, H_2O_2 and Hyp treated cells show a significant 4.5 and 4 fold increased expression when compared to control, the ATSsi + H_2O_2 and ATSsi + Hyp treated cells show a fold change of 2.5 and 2.4 increments when compared to the control group (a and c). DAPI (shown in blue) was used as nuclear stain. n = 3, $p < 0.05$ is considered as significant for differences among groups. Data analysed and expressed as mean ± SD.*]

Adamts4 LOF results in attenuated expression of Periostin. The enhanced expression of periostin observed in H_2O_2 and Hyp treated cells significantly reduced after Adamts knockdown was performed in both ATSsi+ H_2O_2 and ATSsi + Hyp groups (Fig 8 a, b) indicated a Adamts4 mediated functioning of Periostin.

Figure 8

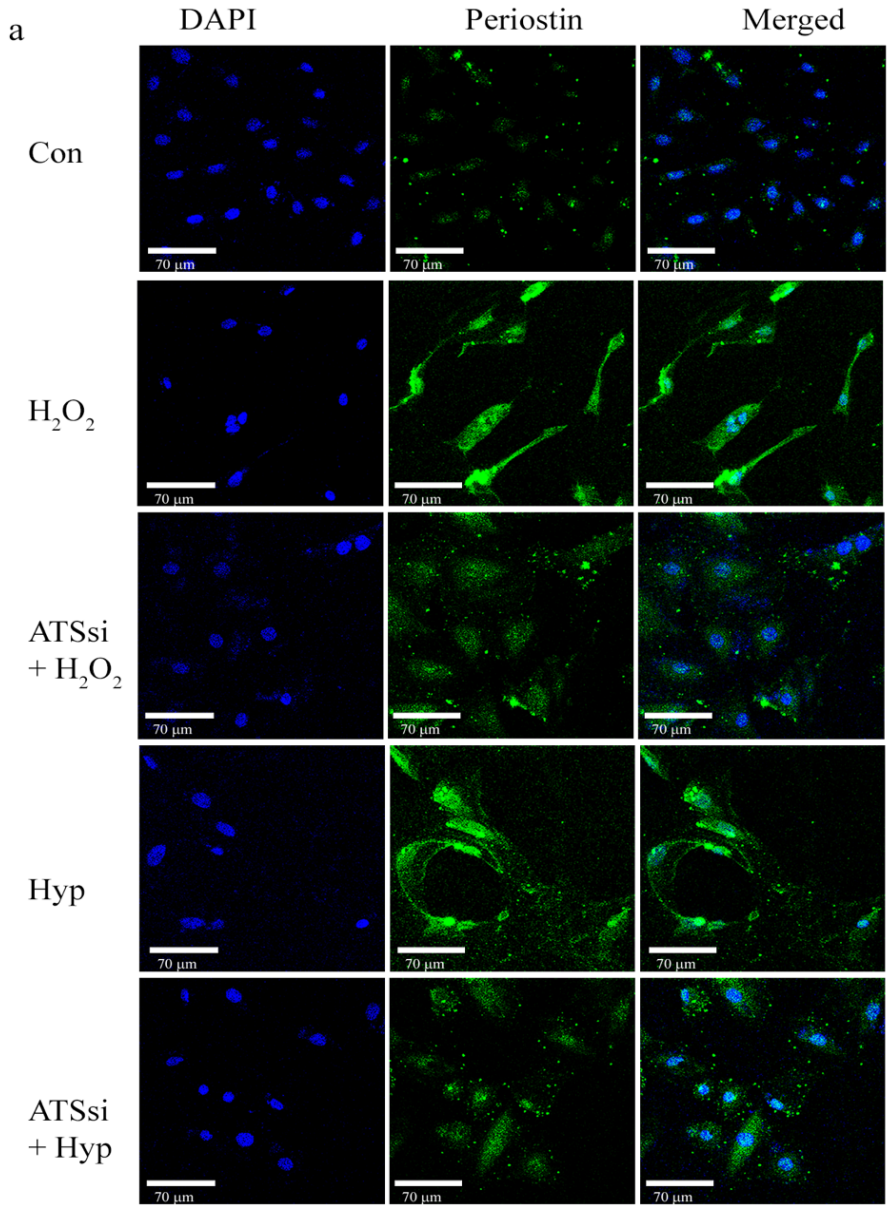

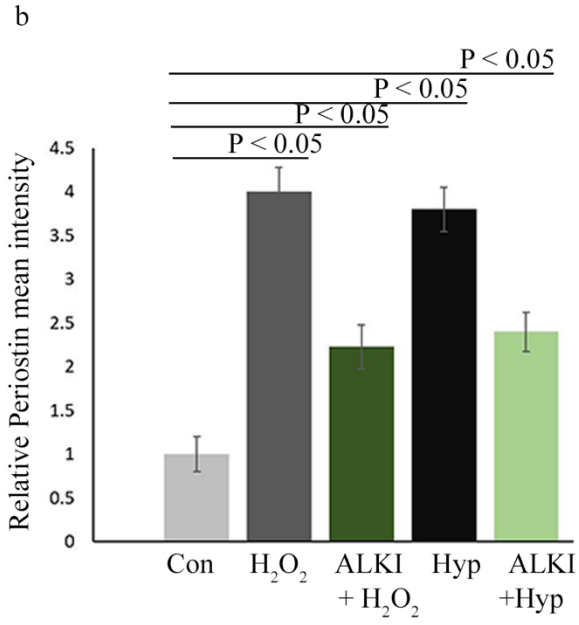

[***Figure 8: Reduced expression of Periostin following Adamts4 loss of function.*** *IF with anti-Periostin antibody (shown in green colour) shows a fold change of 4 and 3.7 increase in the H_2O_2 and Hyp treated group in comparison to the control set, this elevation is significantly reduced 2.4 and 2.2 in ATSsi + H_2O_2 and ATSsi + Hyp groups following siRNA mediated knockdown of Adamts4 (a). DAPI (shown in blue) was used as nuclear stain. Its quantification is depicted in the graph (b). n = 3, data analysed and expressed as mean ± SD. Differences were considered statistically significant for p < 0.05.* **]**

Vimentin over expression in murine adult primary cardiac fibroblasts after ROS and Hypoxia injury. Vimentin, an intermediate filament expressed and associated with fibroblast differentiation to myofibroblast[146] was found to show enhanced expression when the cultured adult murine primary fibroblasts were subjected to ROS and hypoxia injury as compared to control group as shown in panel a of Fig. 9.

Figure 9

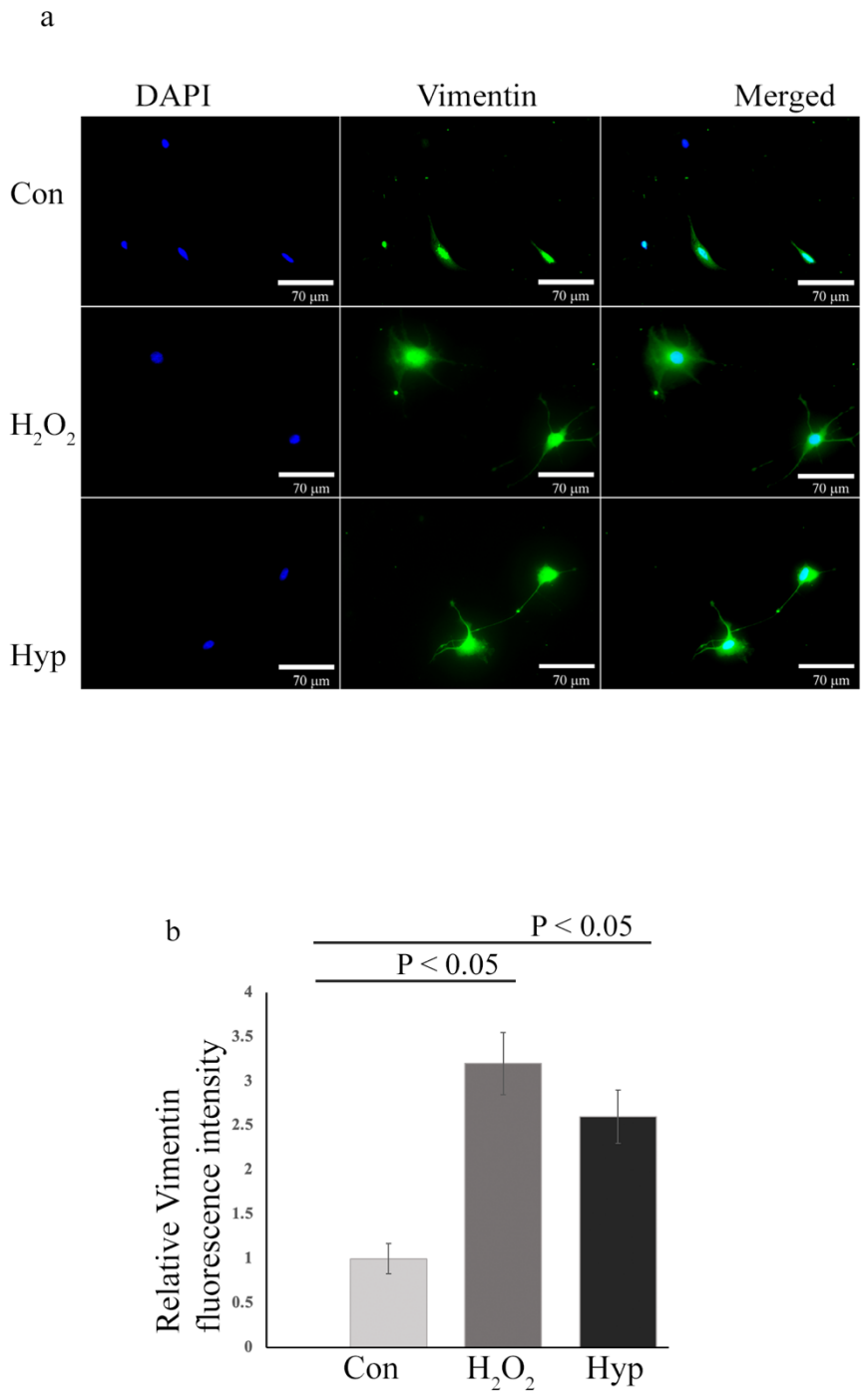

[***Figure 9: Enhanced expression of Vimentin in adult primary cardiac fibroblasts following ROS and hypoxia injury treatment.*** *Staining with anti-Vimentin antibody (shown in green) showed a 3.2 and 2.6 fold change in the mean*

fluorescence intensity of Vimentin post H_2O_2 and hypoxia treatments respectively as compared to control group (a and b). DAPI (in blue) was used as nuclear stain. n=3, data analysed and expressed as mean ± SD. Differences were considered statistically significant for $p < 0.05$. **]**

Upregulation of Periostin and α-SMA in murine adult primary cardiac fibroblasts after ROS and Hypoxia injury. Similar to Vimentin, Periostin and α-SMA marker expressions (measured by mean fluorescence intensities) after immunostaining with the anti-Periostin (Fig. 10a, b) and anti-α-SMA antibodies (Fig. 10 a, c) was found to be significantly upregulated after both injury treatments.

Figure 10

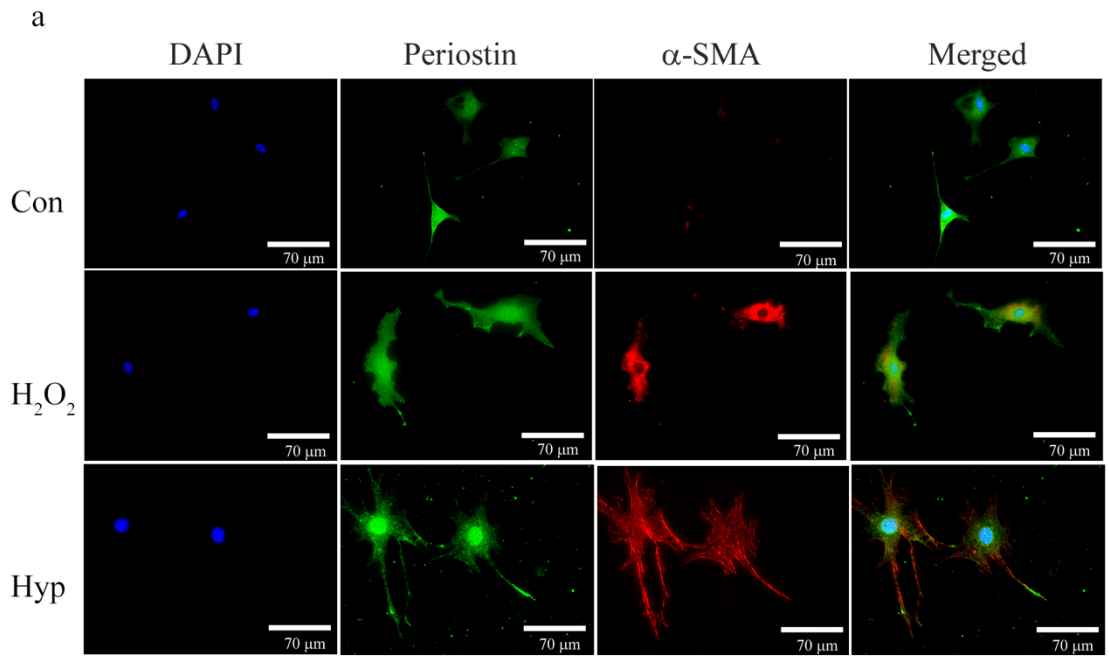

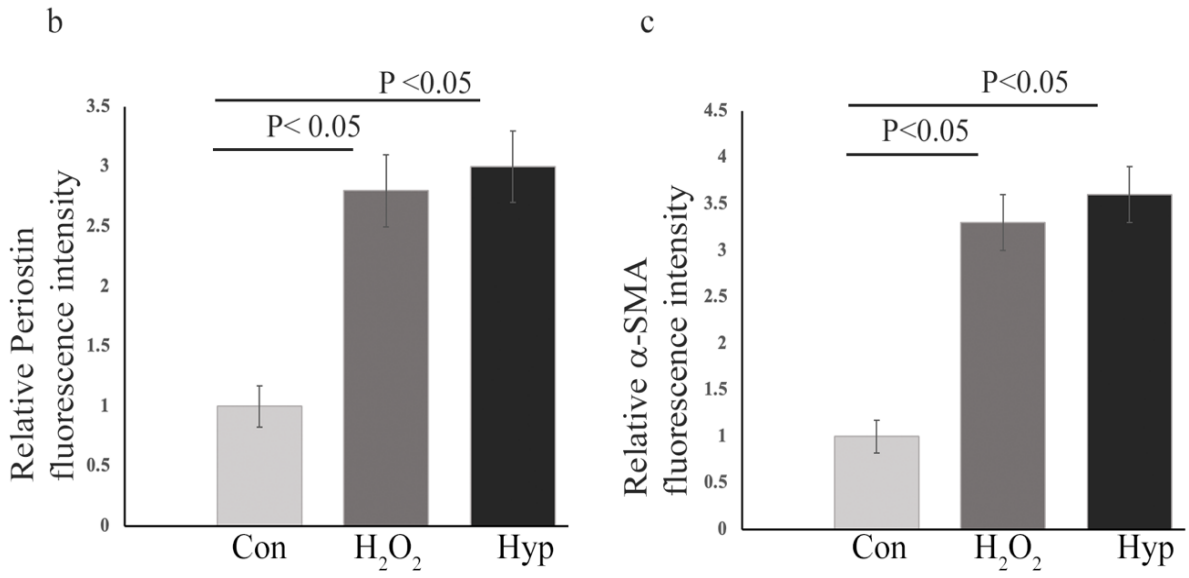

[***Figure 10: Upregulated expression of Periostin and α-SMA in murine adult primary cardiac fibroblasts following ROS and hypoxia injury treatment.*** *Immunostaining with anti-Periostin (shown in green) showed a 2.8- and 3-fold elevation in fluorescence intensity of Periostin in H_2O_2 and hypoxia treated groups as compared to control (a and b) while a 3.3 and 3.6 fold upregulation (in the fluorescence intensity) in the levels of α-SMA (shown in red) was observed for H_2O_2 and hypoxia treated groups respectively (a and c). DAPI (shown in blue) was used as nuclear stain. n=3, data analysed and expressed as mean ± SD. Differences were considered statistically significant for $p < 0.05$.* **]**

Re-activation of Adamts4 and Tgf-β1 in murine adult primary cardiomyocytes after ROS injury. Figure 11a depicts the successful isolation of primary adult mouse cardiomyocytes following culturing under a Differential Interface Contrast (DIC) microscope. Anti-MF20 antibody labeling was used to further confirm the isolation of primary cardiomyocytes (Fig. 11b). Anti-Adamts4 and anti-Tgf-β1 immunostaining revealed upregulation of these two

proteins. (shown in Figs. 11 c, d and e) after ROS induction This finding in primary cardiomyocytes aligns with our findings in cultured H9c2 cells.

Figure 11

a

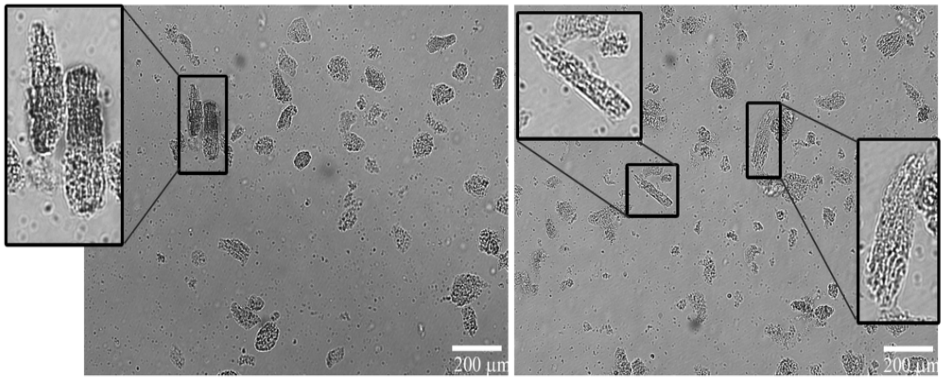

b

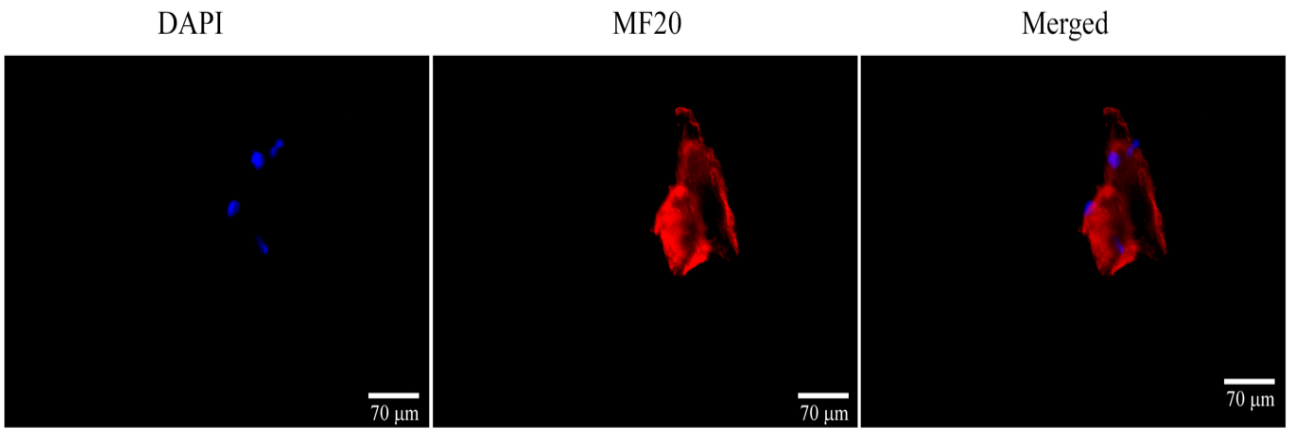

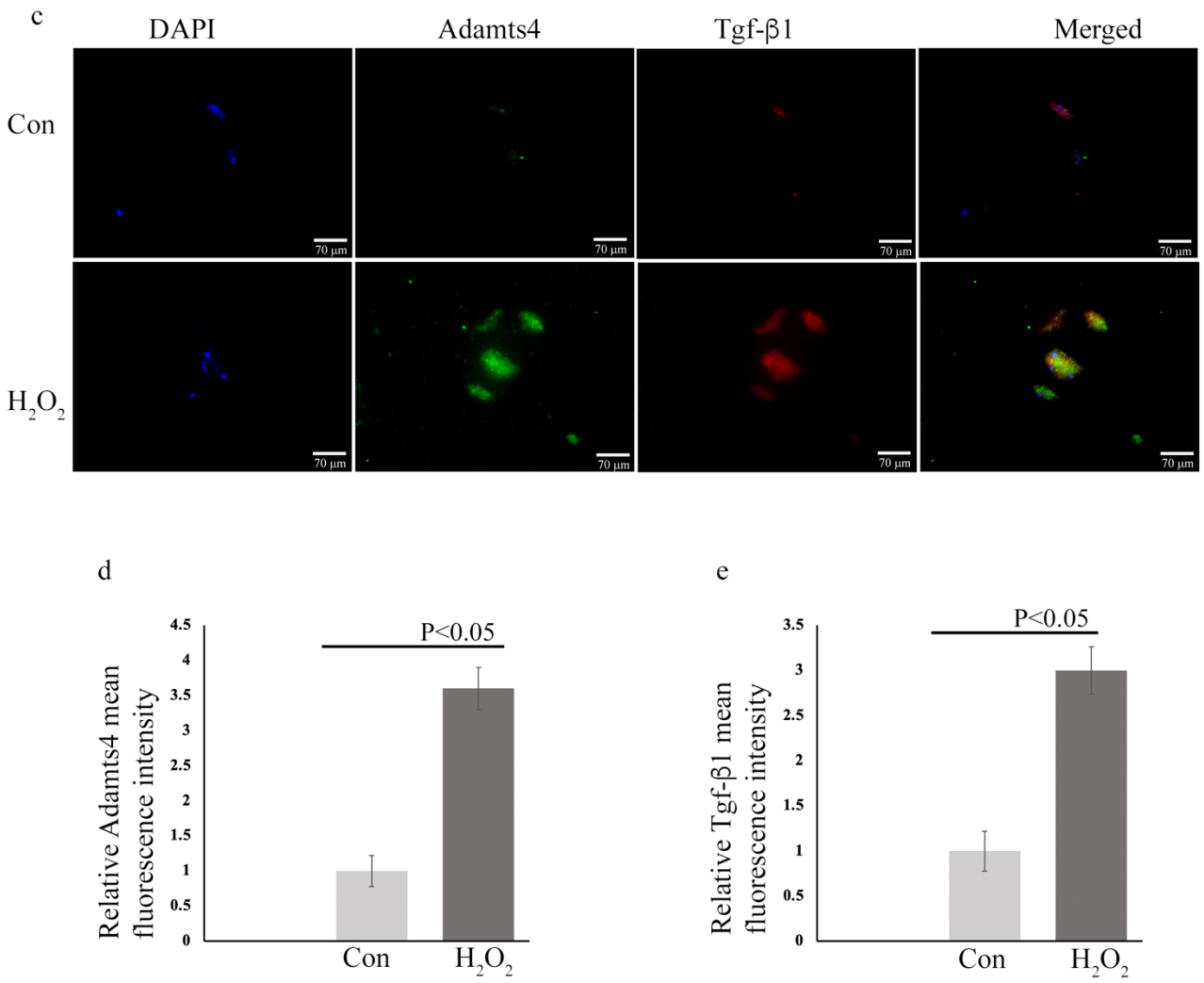

[*Figure 11: Overexpression of Adamts4 and Tgf-β1 in murine adult primary cardiomyocytes after ROS injury.* *The isolation of adult primary cardiomyocytes depicted through DIC images shows the culture status. Few rod shaped cardiomyocytes were observed (insets in a), rest round cardiomyocytes. Further, the isolation was validated with anti-MF20 (shown in red) antibody staining to mark the cardiomyocytes (b). The expression pattern of Adamts4 (shown in green) and Tgf-β1 (shown in red) after H_2O_2 treatment showed a clearly enhanced expression in the fluorescence intensities of both Adamts4 and Tgf-β1 by 3.6 and 3 fold respectively (c, d and e). DAPI (shown in blue) was used as*

nuclear stain. n=3, data analyzed and expressed as mean ± SD. Differences were considered statistically significant for $p < 0.05$. **]**

The induced expression of ADAMTS4 and α-SMA in humans with cardiac anomalies. We used serum samples from human patients who had cardiac abnormalities to better correlate our results in vitro with those in vivo in murine animals. The levels of the proteins ADAMTS4 and α-SMA were determined by western blot. Patients who have experienced MI exhibit increased expression of the proteins ADAMTS4 and α-SMA. The levels of ADAMTS4 in clinical samples of AWMI, IWMI and DCM were assessed by both WB and ADAMTS4 specific ELISA and in both the experiments a significant upregulation of ADAMTS4 was observed in clinical samples (Fig 12a, b and d), so was the expression of α-SMA determined by WB (Fig. 12 a, c). The expression of ADAMTS4 was also found to be elevated similarly in PBMCs (12, e, f) for patients with MI and DCM.

Figure 12

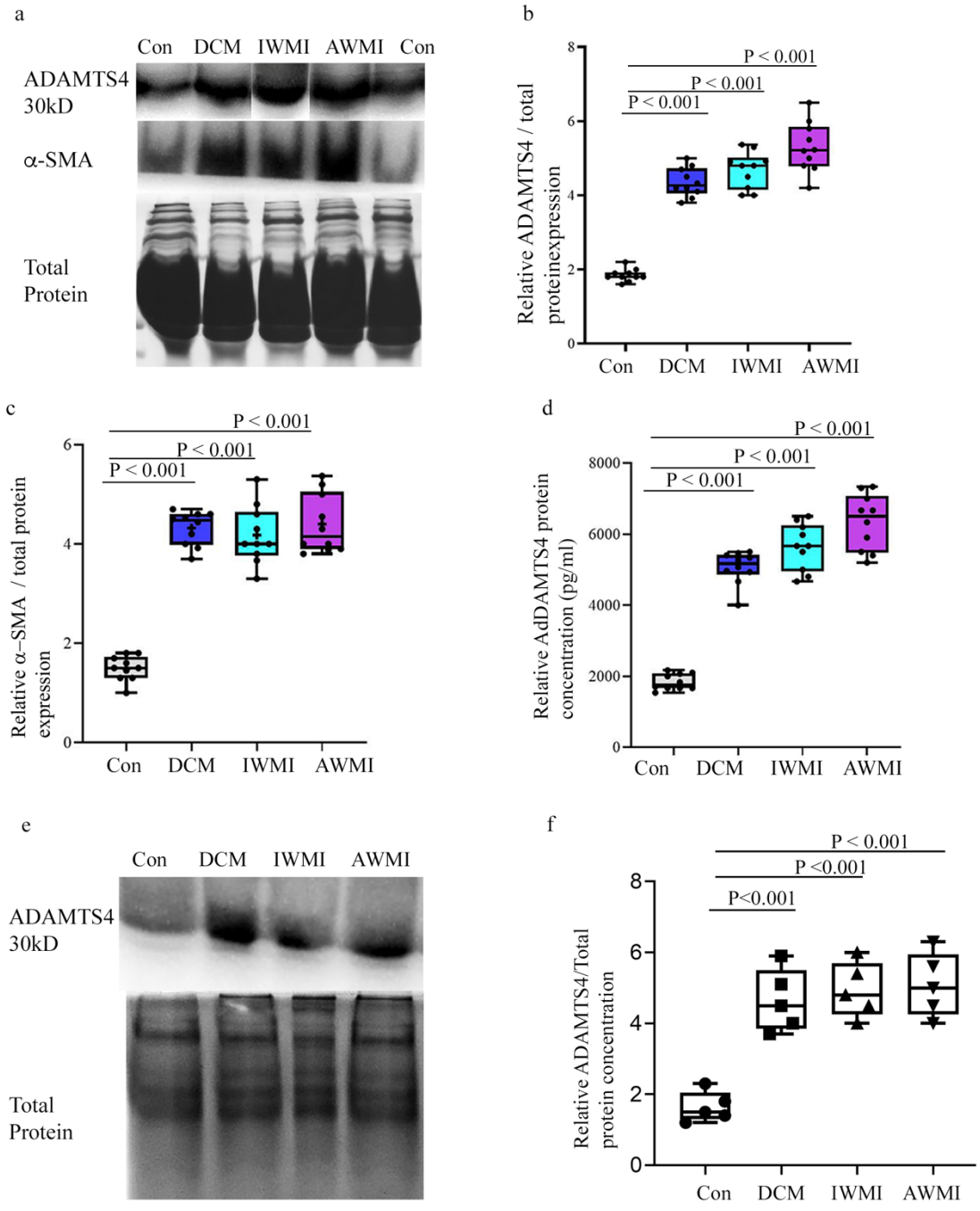
a
Con DCM IWMI AWMI Con
ADAMTS4
30kD
α-SMA
Total
Protein
b
Relative ADAMTS4 / total proteinexpression
P < 0.001
P < 0.001
P < 0.001
Con DCM IWMI AWMI
c
Relative α–SMA / total protein expression
P < 0.001
P < 0.001
P < 0.001
Con DCM IWMI AWMI
d
Relative AdDAMTS4 protein concentration (pg/ml)
P < 0.001
P < 0.001
P < 0.001
Con DCM IWMI AWMI
e
Con DCM IWMI AWMI
ADAMTS4
30kD
Total
Protein
f
Relative ADAMTS4/Total protein concentration
P < 0.001
P <0.001
P<0.001
Con DCM IWMI AWMI

[***Figure 12: Upregulation of ADAMTS4 and α-SMA proteins in adult cardiac patients.*** *ADAMTs4 and α-SMA WB data of affected cardiac patients and control (a), its quantification (b and c). An elevated expression of ADAMTS4 varying from 3 to 4.5 folds for patients with DCM, 4 to 5.3 folds for IWMI patients and 4 to 6.5 for patients with AWMI and varying in comparison to the control group (with no indicated cardiac abnormalities), where the expression fold varies from 1.6 to 2.3 fold. (a and b) was observed. The same was true for α-SMA which showed increased fold change varied from 3.7 to 4.7, 3.3 to 5.3, 3.9 to 5.4 for DCM, IWMI, and AWMI groups in comparison with the control set where fold levels for α-SMA varied from 1 to 1.8. (a and c). Total protein was used as loading control. Further, ADAMTS4 specific ELISA showed concentration gradient varying from 4666 to 6500 (pg/ml), 5200 to 7333 (pg/ml), and 4000 to 5500 (pg/ml) for DCM, IWMI, and AWMI groups respectively as compared to the concentration gradient observed for the control group which varied from 1533 to 2170 (pg/ml) (d). (n=5 for WB for each group, N=10 and n=2 for ELISA for each study group). The proposed model (e) shows ADAMTS4 WB in PBMCs isolated from clinical samples and the quantified upregulated expression is depicted in panel f. Expression of ADAMTS4 ranged from 3.8 to 5.8 fold for DCM samples, 4-5.9 folds for IWMI and 4 to 6.2 folds for AWMI samples in comparison to 1.5-2.3 fold expression found in control groups. N=5 for PBMC samples. Data analysed and expressed as median, 1st and 3rd quartile and range. $p < 0.05$ was considered a significant difference.* **]**

Adamts4 expression following hyperglycaemic shock in H9c2 cells. Following glucose shock treatment to mimic diabetic cardiomyopathic like environment, qPCR assay (Fig 13, a, b, c and d) for the expression of Glut-1, Collagen-III, α-SMA and Adamts4 was done and WB for Adamts4 (13 d and e) was performed. Upregulated Glut-1 mRNA levels showed successful hyperglycaemic induction in cells treated with 20mM glucose compared with the 5mM treated control group while elevated Col-III mRNA and α-SMA mRNA expression hinted at the ECM remodeling undertone. Finally elevated expression of Adamts4 expression determined by both qPCR and WB suggests Adamts4 to be a key regulator of ECM remodeling in hyperglycaemic conditions as well.

Figure 13

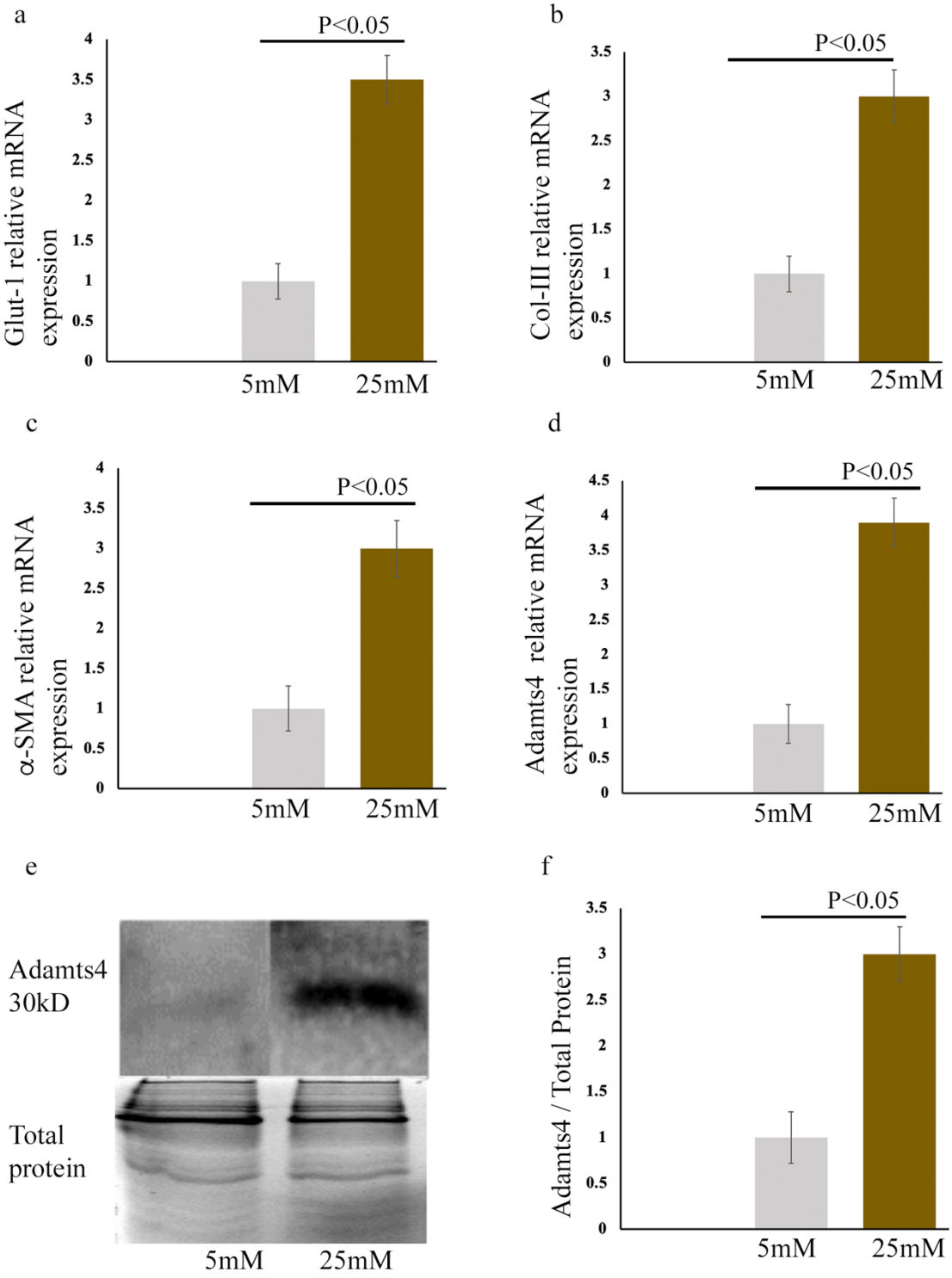

[*Figure 13: Adamts4 expression following hyperglycaemic shock in H9c2 cells.* *Following glucose shock treatment, qPCR assay (a, b , c and d) for the expression of Glut-1, Collagen-III, α-SMA and Adamts4 mRNA was done and*

WB for Adamts4 protein (e and f) was performed. Glut-1 mRNA levels were found to be 3.5 fold elevated in cells treated with 20mM glucose in compared with the 5mM treated control group while Col-III mRNA expression was found to increase 3 fold in the treatment group. Similarly α-SMA levels were also significantly elevated by 3 folds in glucose treated cells. Finally Adamts4 expression was found to be 3.9 and 3 fold observed by qPCR and WB assay respectively (c, d and e). n=3, data analyzed and expressed as mean ± SD. Differences were considered statistically significant for $p < 0.05$. **]**

Assessment of Fasting blood glucose (FBG), serum triglycerides and cholesterol in high fat diet along with alloxan treated rats along with expression of ADAMTS4 in clinical samples of DCM with T2D (DCM&D).

FBG was measured over the course of the rats being fed with High fat diet and thereafter treated with alloxan monohydrate in the were recorded over a period of 9 weeks. The FBG (Fig. 14 a) of high fat diet rats (T1, T2 & T3) followed by alloxan treatment were elevated (a) so were the serum cholesterol and triglyceride levels (shown in table 2). Finally ADAMTS4 expression was also conducted in serum samples of patients with DCM along with T2D (DCM&D) by ADAMTS4 specific ELISA. Adamts4 expression were found to be significantly upregulated in clinical diabetic samples when compared with the control group (Fig. 14b).

Figure 14

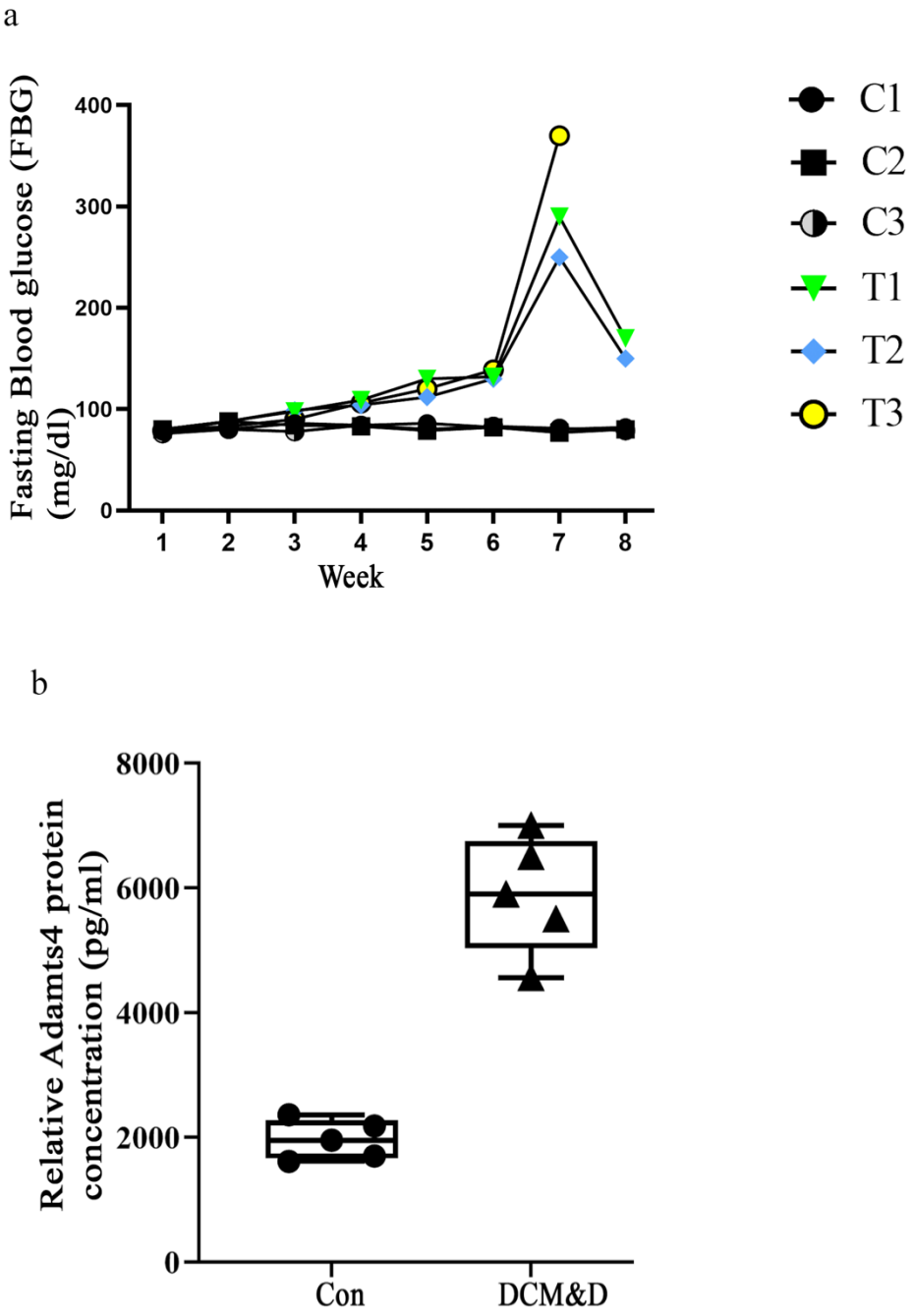

[***Figure 14: Measurement of FBG, in T2D induced rats along with measurement of ADAMTS4 in DCM&D samples.*** *FBG over the course of the rats being fed with High fat diet and thereafter treated with alloxan monohydrate in the were recorded over a period of 9 weeks. Unfortunately, 2 of the 3 alloxan treated rats failed to survive after alloxan treatment. The FBG of high fat diet*

rats followed by alloxan treatment were elevated (a) ranging from 80 to 400 mg/dl compared to the control group were variation was 78-90 mg/dl over a period of 8 weeks (6 weeks of HFD + alloxan treatment and follow up in the next 2 weeks). Finally ADAMTS4 expression was also conducted in serum samples of patients with DCM along with T2D (DCM&D) by WB. Adamts4 expression assessed by ADAMTS4 specific ELISA were found to be varying between 4500 pg/ml to 7000 pg/ml in comparison to the control group where the concentration ranged from 1600 to 2300 pg/ml (b) n=3 for in-vivo samples and n=5 for clinical samples. p<0.05 was considered statistically significant. Data analysed and expressed as median ± SD. **]**

Table 2:

	Cholesterol (mg/dl)	**Triglyceride (mg/dl)**
C1	78	72
C2	76	73
C3	75	76
T1	112	105
T2	115	109
T3	102	100

Table 2: *Cholesterol and Triglyceride levels of control (C1, C2 and C3) and High fat+ Alloxan treated rats (T1, T2 and T3)*

D. Discussion

This study's key discovery is that cardiac muscle damage upregulates Adamts4. This result is in line with earlier research that demonstrated increased Adamts4 expression in atherosclerotic plaques[41] and patients with acute coronary syndrome.[43] Importantly, Adamts4 functions to control the turnover of other proteins by directly influencing other resident cells, including but not limited to cardiac fibroblasts, endothelial, and smooth muscle cells in the same ECM milieu. Adamts4 is a secretory protein that resides both intracellularly and is also secreted from cardiomyocytes out into the ECM. It is uncertain how Adamts4 is activated by damage in other adult cardiac resident cell types. Adamts4 was easier to experiment with within H9c2, a cardiomyocyte cell line. Injury inductions through H_2O_2 and hypoxia treatment showed upregulation of Adamts4 along with a couple of other fibrosis-related markers like Tgf- β1, Collagen-III, α-SMA, and Periostin which is notably known as a marker for detecting fibroblast to myofibroblast switch[93] were found to be elevated (Fig. 2) implying that an injury mediated ECM remodeling could be a cause for the elevation of these markers. Further pre-treatment with SB431542, an inhibitor of ALK4 and 5 (one of the two binding receptors of Tgf- β1) receptor that eventually leads to inhibition of Tgf- β1 also showed inhibition of Adamts4, this inhibition further extended to the expression of Collagen-III, α-SMA and Periostin proteins (Figs. 3, 4 and 5). To better understand the hierarchy supremacy between Adamts4 and Tgf- β1, Adamts4 loss of function study was mediated by Adamts4 siRNA transfection. In groups where Adamts4 knockdown was performed before stress induction, Tgf- β1 expression remained quite unaffected whereas the expression of the other 3 mentioned markers- Collagen-III, α-SMA, and Periostin along with Adamts4 was found to reduce to somewhat similar levels when ALKI pre-treatment with stress induction was done (Figs. 6,7 and 8). These findings indicated that Adamts4 expression is mediated by Tgf- β1 and also that other ECM and fibrosis

related markers including Col-III, α-SMA, and Periostin seem to be regulated by Adamts4 since loss of function of Adamts4 significantly inhibited the expression of these markers following injury to H9c2 cells. Moreover, isolated adult primary mice cardiac fibroblasts showed the same effect, i.e., enhanced expression of Vimentin (Fig 9), α-SMA, and Periostin (Fig. 10 a, b) confirmed a fibrosis like scenario while isolation of adult primary mice cardiomyocytes showed enhanced expression of both Tgf-β1and Adamts4 (Fig. 11 c, d and e) indicating the effector role of Adamts4 (a secretory matrix component) on the cardiac fibroblasts. Finally, not only our marker of interest, ADAMTS4 but also α-SMA showed significantly enhanced expression in patients with MI and DCM injury (Fig. 12) indicating a cardiac fibrosis like condition following adult cardiac injury. Future research aimed at confirming the direct interaction of Adamts4 with Col-III -SMA and Periostin by binding/ChIP assays would provide insight into how Adamts4, Periostin, and -SMA interact. Additionally, the expression Glut-1, Adamts4 along with fibrosis markers like Col-III , α-SMA in H9c2 cells treated with high glucose shows the involvement of Adamts4 in ECM remodeling in conditions of diabetic cardiomyopathy (Fig. 13). Furthermore, animal models subjected with high fat diet followed by alloxan treatment to induce T2D showed a rise in FBG levels (Fig. 13 a) (but the levels could not be sustained unfortunately and other experimental cohorts could not be experimented with owing to the COVID-19 pandemic) and a prolife hinting of progression of dyslipidaemia (Table. 2). Ultimately, expression of ADAMTS4 in patients with DCM in addition to T2D showed even more elevated expression of ADAMTS4 (Fig. 14 b) than expressed in DCM patients alone suggestive of ADAMTS4 mediated ECM remodeling and fibrosis might be pivotal in pathophysiology of such cases. The ECM is an integral part of the myocardium. The ECM in the heart is composed of a dynamic mixture of proteins, including collagen, elastin, fibronectin, and proteoglycans. It provides structural stability and elasticity to

cardiac tissue and helps maintain the normal functioning of cardiomyocytes, the contractile cells of the heart. The ECM also influences cell signaling, migration, and proliferation, making it a key player in tissue remodeling during development, aging, and disease. The dynamic composition of cardiac ECM consisting of both structural and non-structural components plays a critical role in cellular events and during pathogenicity[147,148]. Under stress conditions such as Ischemia or MI, the chamber myocardium undergoes intensive ECM remodeling which remains relatively inconspicuous in healthy individuals. Cardiac Fibrosis is often viewed as an expansion of ECM remodeling[149]. Following MI or I/R, there is an acute inflammatory response that suffices for the overexpression of pro-inflammatory cytokines like Tgf- β and interleukins. Tgf- β1 most notably does so by the canonical Smad 2/3 signaling cascade which leads to fibrosis.[44,45,149] Tgf-β stimulates the production of ECM components, such as collagen and fibronectin, by activating specific signaling cascades in cardiac fibroblasts. This leads to ECM accumulation, promoting tissue repair and scar formation in response to injury or stress . This signaling cascade activates certain MMPs like Adamts[150,151] family among others as a part of the pro-inflammatory mediated cell signaling cascade and these MMPs then take over the centre stage post-cardiac injury such as MI which leaves behind a pool of necrotic myocytes, it is then that the MMPs like Adamts4 takeover to regulate a turn-over in the synthesis of matrix macromolecules like Collagen-I/III, α-SMA, and Periostin, Tenascin-C to synthesize more matrix macromolecules and fibroblasts which is required to fill in the scar left by necrosis of myocardial cells in order to maintain the physiology of the myocardium since adult cardiomyocytes have very limited proliferation capacity. Periostin is very commonly found significantly elevated in patients with MI and hypertrophic cardiomyopathy and is one of the key contributors of fibrosis. However, prolonged expansion of ECM could lead to extensive fibrosis. Fibrosis stiffens the myocardium, impairs contractile function, disrupts electrical conduction, and promotes arrhythmias. Hyperglycaemia-induced activation of

various pathways, including advanced glycation end products (AGEs), protein kinase C (PKC), and transforming growth factor-beta (TGF-β), play crucial roles in ECM alterations. AGEs promote collagen cross-linking and fibrosis, while PKC activation stimulates ECM synthesis and inhibits degradation. Moreover, pathological ECM remodeling alters cell signaling, exacerbates inflammation, and contributes to maladaptive cardiac remodeling. and as a resulting stiffness of the myocardium following which ventricular dysfunction could occur which itself may turn fatal and thus inhibition of MMPs like Adamts4 could be one of the possible targets to reduce fibrosis post-cardiac injury[152] like the one proposed in our model (Fig. 15) by inhibiting Tgf- β1.

To conclude, the work shows Adamts4 is upregulated in response to cardiac stress *in-vitro* and in human studies. Further this upregulated expression of Adamts4 is under the regulation of Tgf-β1. The routinely studied biomarker of cardiac injury are Troponin-T and Creatine kinase. Since our work shows that Adamts4 governs the expression of other ECM and fibrosis promoting markers like Col-III, Periostin and α-SMA, Adamts4 regulates the overall cardiac health and functioning and it could open doors for therapeutic approaches to target Adamts4 for manipulating cardiac health. As our data shows the hallmark expression of Adamts4 in cardiac stress conditions, it can be considered as a novel biomarker for cardiac related injuries leading way for therapeutics to manipulate its expression following cardiac injury for improvement of cardiac functioning. With the promising future of cardiac targeting peptides, it could be possible to specifically target Adamts4 via peptides loaded with Adamts4 siRNA or inhibitor to specifically target the myocardium in cases of MI to prevent the deteriorating condition of the myocardium following an infarction.